Effective field theories and cosmological scattering equations

C. Armstrong,[a] H. Gomez,[a,b] R. Lipinski Jusinskas,[c] A. Lipstein[a] and J. Mei[a]

[a]*Department of Mathematical Sciences, Durham University,*
Stockton Road, DH1 3LE, Durham, United Kingdom

[b]*Facultad de Ciencias Basicas, Universidad Santiago de Cali,*
Calle 5 N° 62-00 Barrio Pampalinda, Cali, Valle, Colombia

[c]*Institute of Physics of the Czech Academy of Sciences & CEICO,*
Na Slovance 2, 182 21, Prague, Czech Republic

E-mail: connor.armstrong@durham.ac.uk, humberto.gomez@durham.ac.uk,
renannlj@fzu.cz, arthur.lipstein@durham.ac.uk,
jiajie.mei@durham.ac.uk

Abstract: We propose worldsheet formulae for wavefunction coefficients of the massive non-linear sigma model (NLSM), scalar Dirac-Born-Infeld (DBI), and special Galileon (sGal) theories in de Sitter momentum space in terms of the recently proposed cosmological scattering equations constructed from conformal generators in the future boundary. The four-point integrands are assembled from simple building blocks and we identify a double copy prescription mapping the NLSM wavefunction coefficient to the DBI and sGal wavefunction coefficients, including mass deformations and curvature corrections. Finally, we compute the soft limits of these wavefunction coefficients and find that they can be written in terms of boundary conformal generators acting on contact diagrams.

Contents

1 Introduction

In recent years, there has been exciting progress in adapting methods for computing scattering amplitudes, which probe physics at its shortest distances, to cosmological observables, which probe physics at its largest distances. In the latter, we have in mind boundary correlators in four dimensional de Sitter space (dS$_4$), which provides an approximate description of the early Universe according to the inflationary paradigm [1–4]. The cosmological observables we focus on are known as coefficients of the wavefunction of the universe [5]. They are computed via a Wick rotation of Witten diagrams in Anti de Sitter (AdS) and

can be treated like conformal field theory (CFT) correlators in the future boundary of dS [6–12]. In-in correlators [13] can then be computed by squaring of the wavefunction and computing expectation values [7]. Recent developments in this direction include geometric approaches [14, 15], methods based on factorisation [16–20] and unitarity [21–28], Mellin-Barnes representations [29, 30], color/kinematics duality [31–38], the double copy [39–42], and the cosmological scattering equations (CSE) [43, 44]. See also [45–48] for other recent work adapting amplitude ideas to (A)dS correlators.

Here we focus on the double copy and the CSE. In flat space, the double copy relates graviton amplitudes to the square of gluon amplitudes [49, 50], and the scattering equations of Cachazo, He, and Yuan (CHY) [51, 52] provide a universal framework for describing scattering amplitudes in terms of worldsheet integrals [53–55]. They uncover a vast web of relations among quantum field theories such as the non-linear sigma model (NLSM), Dirac-Born-Infeld (BDI), and special Galileon (sGal) theories, extending the scope of the double copy [56–58]. The CSE represent an extension of the flat space scattering equations to de Sitter momentum space. They were initially proposed to describe massive ϕ^4 theory as a toy model of inflation, building on earlier work on bi-adjoint scalar theory in AdS position space [59, 60]. One of the key properties of this proposal is an operatorial integrand built out of conformal generators in the future boundary of dS which acts on a contact diagram. An important open question was how to extend this structure to more general scalar theories, and here we take the first steps to address it.

Towards this goal, we will extend the CSE framework to the NLSM, scalar DBI, and sGal theories in dS space. When lifting derivative interactions to curved background, new subtleties arise. First of all, the spacetime Lagrangians receive curvature corrections whose coefficients cannot be fixed by the flat space limit. At four points, we find that such corrections can be described using simple building blocks at the level of the worldsheet integrand. We can also deform the integrand to describe bulk scalar fields with arbitrary mass. The other class of subtleties is related to more technical aspects of the problem. Becasue of derivative interactions in the curved background, the worldsheet formulae may have ordering ambiguities involving differential operators with nontrivial commutators. Such ambiguities can arise in the NLSM at six points and the DBI and sGal theories at four points, although we use a simple prescription for avoiding them at four points.

Our worldsheet formulae give rise to four-point wavefunction coefficients in terms of boundary conformal generators acting on contact diagrams. We also identify a simple prescription for mapping the NLSM wavefunction coefficient into the DBI and sGal wavefunction coefficients at the level of the worldsheet integrand, which we refer to as a generalised double copy. After specifying a prescription for evaluating the worldsheet integrals to avoid ordering ambiguities, this provides a systematic way to implement the double copy of four-point wavefunction coefficients in these theories. Finally, we study the soft limits of the four-point wavefunction coefficients and find that they can once again be written in terms of boundary conformal generators acting on certain three-point contact diagrams. In the flat space limit, the scattering amplitudes of these theories are well-known to exhibit vanishing soft limits [61, 62] as a result of underlying hidden symmetries [63–65]. In our treatment, the coefficients of curvature corrections are left unfixed and the soft limits we

derive are completely general. Lagrangians for the DBI and sGal theories with certain hidden symmetries in dS were recently proposed in [66]. It would be interesting to compute their four-point wavefunction coefficients in terms of the building blocks we derive in this paper and check if their soft limits exhibit any additional simplicity. Soft limits of flat space wavefunction coefficients in these theories were also recently analysed in [67].

This paper is organised as follows. In section 2 we review the NLSM, DBI, and sGal theories in flat space and the CHY representation for their amplitudes. In section 3, we then discuss how to lift these theories to dS space up to four-point interactions, and compute their four-point wavefunction coefficients in terms of Witten diagrams. In section 4, we then propose worldsheet formulae for these wavefunction coefficients in terms of CSE, and a generalised double copy which maps the NLSM wavefunction coefficient into the DBI and sGal wavefunction coefficients, including curvature corrections and mass deformations. In section 5, we analyse the soft limits of these four-point wavefunction coefficients and show that they can be written in terms of boundary conformal generators acting on certain three-point contact diagrams. We present our conclusions in section 6. We also have a number of appendices in which we compute wavefunction coefficients for the six-point NLSM in dS using Witten diagrams and worldsheet methods, and provide more details on four-point wavefunction coefficients.

2 Effective field theory amplitudes

In this work we focus on certain scalar effective field theories (EFT), namely the non-linear sigma model (NLSM), scalar Dirac-Born-Infeld theory (DBI), and special Galileon theory (sGal). Their scattering amplitudes take a particularly simple form in the CHY approach [56].

2.1 Lagrangians

We start with a quick review of the scalar EFT Lagrangians.

The NLSM Lagrangian is given by

$$
\begin{aligned}
\mathcal{L}_{\text{NLSM}} &= \frac{1}{8\lambda^2} \text{Tr}(\partial_\mu U^\dagger \partial^\mu U), \\
&= -\text{Tr}\left[\tfrac{1}{2}\partial_\mu \Phi \partial^\mu \Phi + \lambda^2 \Phi^2 \partial_\mu \Phi \partial^\mu \Phi + \lambda^4 \left(\Phi^4 \partial_\mu \Phi \partial^\mu \Phi + \tfrac{1}{2}\Phi^2 \partial_\mu \Phi \Phi^2 \partial^\mu \Phi\right) + \ldots\right],
\end{aligned}
\tag{2.1}
$$

where $U = (\mathbb{I} + \lambda\Phi)(\mathbb{I} - \lambda\Phi)^{-1}$, Φ is in the adjoint representation of $\text{SU}(N)$, and the ellipsis denotes higher-point interactions. For the DBI theory we have

$$
\begin{aligned}
\mathcal{L}_{\text{DBI}} &= \frac{1}{\lambda}\left(\sqrt{1 - \lambda\left(\partial\phi\right)^2} - 1\right), \\
&= -\frac{1}{2}\partial\phi \cdot \partial\phi - \frac{\lambda}{8}\left(\partial\phi \cdot \partial\phi\right)^2 + \ldots.
\end{aligned}
\tag{2.2}
$$

Finally, in $d = 4$ the special Galileon theory is given by [64]

$$
\mathcal{L}_{\text{sGal}} = -\frac{1}{2}\left(\partial\phi\right)^2 - \frac{\lambda}{8}\left(\partial_\mu \partial_\nu \phi\right)^2 \left(\partial\phi\right)^2.
\tag{2.3}
$$

Theory	Integrand
NLSM	$\mathrm{PT}(\mathrm{Pf}'A)^2$
DBI	$\mathrm{Pf}X(\mathrm{Pf}'A)^3$
sGal	$(\mathrm{Pf}'A)^4$

Table 1. A summary of CHY integrands for a selection of scalar EFTs.

Note that the four-point interactions in the DBI and sGal theories contain four derivative and six-derivatives, respectively. They are unique up to integration by parts and equations of motion. Their lift to curved backgrounds, however, is not unique because covariant derivatives no longer commute and there are curvature corrections, as we describe later on.

2.2 Worldsheet formulae

The CHY formulae express tree-level scattering amplitudes as integrals over the Riemann sphere, which localise onto solutions of the scattering equations (SE),

$$S_a = \sum_{a \neq b} \frac{2\, k_a \cdot k_b}{\sigma_{ab}} = 0, \qquad \sigma_{ab} \equiv \sigma_a - \sigma_b, \tag{2.4}$$

where σ_a is the holomorphic coordinate of the a-th puncture, and the punctures are in one-to-one correspondence with the external legs of the amplitude. The details of the theory appear only in the worldsheet integrand, and a generic n-point tree level amplitude takes the form

$$\mathcal{A}_n = \int_\gamma \prod_{\substack{a=1 \\ a \neq b,c,d}}^n \mathrm{d}\sigma_a \, (S_a)^{-1} \, (\sigma_{bc}\sigma_{cd}\sigma_{db})^2 \, \mathcal{I}_n, \tag{2.5}$$

where $\{b, c, d\}$ are fixed punctures. The integration contour is defined by the intersection $\gamma = \bigcap_{a \neq b,c,d} \gamma_{S_a}$, where γ_{S_a} encircles the poles of S_a.

The CHY integrands for the scalar EFTs of interest are defined using simple building blocks, with various operations to transform between different theories [56]. They are summarised in table 1 and we will briefly review their construction.

The integrand for color-ordered amplitudes of the NLSM is

$$\mathcal{I}^{\mathrm{NLSM}}(\alpha_1, \alpha_2, \ldots, \alpha_n) = \mathrm{PT}(\alpha_1, \alpha_2, \ldots, \alpha_n)(\mathrm{Pf}'\mathrm{A})^2, \tag{2.6}$$

where $\alpha = (\alpha_1, \alpha_2, \ldots, \alpha_n)$ denotes a specific ordering, and PT is the Parke-Taylor factor

$$\mathrm{PT}(\alpha_1, \alpha_2, \ldots, \alpha_n) = (\sigma_{\alpha_1\alpha_2}\sigma_{\alpha_2\alpha_3} \cdots \sigma_{\alpha_n\alpha_1})^{-1}. \tag{2.7}$$

In practice we will use the canonical ordering, i.e. $\mathrm{PT}(1, 2, \ldots, n)$, so for simplicity we introduce the notation

$$\mathrm{PT} \equiv \mathrm{PT}(1, 2, \ldots, n). \tag{2.8}$$

The reduced Pfaffian $\mathrm{Pf}'A$ is given by

$$\mathrm{Pf}'A = \frac{(-1)^{c+d}}{\sigma_{cd}} \mathrm{Pf} A_{cd}^{cd}, \tag{2.9}$$

$$\mathrm{Pf} A_{cd}^{cd} = \frac{\epsilon^{r_1 s_1 \ldots r_{p-1} s_{p-1}} (A_{cd}^{cd})_{r_1 s_1} \cdots (A_{cd}^{cd})_{r_{p-1} s_{p-1}}}{2^{p-1}(p-1)!}, \tag{2.10}$$

where the matrix A_{cd}^{cd} is obtained from the $n \times n$ matrix

$$A_{rs} = \begin{cases} \dfrac{2k_r \cdot k_s}{\sigma_{rs}}, & r \neq s, \\ 0, & r = s, \end{cases} \tag{2.11}$$

by removing any pair of rows and columns $\{c, d\}$, with $n = 2p$. Alternatively the Pfaffian can be computed from the square root of the determinant.

For the scalar DBI theory, the worldsheet integrand is given by

$$\mathcal{I}^{\mathrm{DBI}} = \mathrm{Pf} X (\mathrm{Pf}'A)^3, \tag{2.12}$$

where

$$X_{rs} = \begin{cases} \dfrac{1}{\sigma_{rs}}, & r \neq s, \\ 0, & r = s. \end{cases} \tag{2.13}$$

The X-matrix arises from dimensional reduction of the CHY formula for Yang-Mills amplitudes [56]. These reason for this will be further explained below. Finally, the integrand for the sGal theory is given by

$$\mathcal{I}^{\mathrm{sGal}} = (\mathrm{Pf}'A)^4. \tag{2.14}$$

Observe that the integrands of both DBI and sGal can be obtained from NLSM via the following substitutions, respectively:

$$\mathrm{PT} \to \mathrm{Pf} X (\mathrm{Pf}'A), \tag{2.15}$$

$$\mathrm{PT} \to \left(\mathrm{Pf}'A\right)^2, \tag{2.16}$$

which encode the double copy structure of these theories. Roughly speaking, sGal = NLSM^2 and DBI = NLSM $\times$ YM, where YM corresponds to the dimensional reduction of Yang-Mills theory. More precisely, $\mathrm{Pf} X (\mathrm{Pf}'A)$ can be written as a linear combination of $(n-2)!$ Parke-Taylor factors, where the coefficients are the Yang-Mills BCJ master numerators after the identification $\epsilon_i \cdot \epsilon_j = 1$ and $\epsilon_i \cdot k_j = 0$ [54, 56, 58, 68–72].

3 de Sitter wavefunction coefficients from effective actions

In this section we review the computation of field theory observables in de Sitter. For convenience, we use the Poincaré patch with radius set to one,

$$ds^2 = \frac{1}{\eta^2}(d\vec{x}^2 - d\eta^2), \tag{3.1}$$

where $-\infty < \eta < 0$ is the conformal time, and $\vec{x}$ denotes the boundary coordinate, with individual components x^i, $i = 1, \ldots, d$. In practice, we set the dimension of the boundary $d = 3$.

In-in correlators [13] can be computed from a cosmological wavefunction as follows [7]:

$$\langle \phi(\vec{k}_1) \ldots \phi(\vec{k}_n) \rangle = \frac{\int \mathcal{D}\phi \, \phi(\vec{k}_1) \ldots \phi(\vec{k}_n) \, |\Psi[\phi]|^2}{\int \mathcal{D}\phi \, |\Psi[\phi]|^2}. \tag{3.2}$$

The scalars ϕ are taken to be in the future boundary, Fourier transformed to momentum space. The functional $\Psi[\phi]$ is the cosmological wavefunction, which can be perturbatively expanded as

$$\ln \Psi[\phi] = -\sum_{n=2}^{\infty} \frac{1}{n!} \int \prod_{i=1}^{n} \frac{\mathrm{d}^d k_i}{(2\pi)^d} \Psi_n(\vec{k}_1, \ldots, \vec{k}_n) \phi(\vec{k}_1) \ldots \phi(\vec{k}_n). \tag{3.3}$$

The wavefunction coefficients Ψ_n can be treated as n-point CFT wavefunction coefficients in the future boundary. In momentum space, they can be expressed as

$$\Psi_n = \delta^d(\vec{k}_T) \langle\langle \mathcal{O}(\vec{k}_1) \ldots \mathcal{O}(\vec{k}_n) \rangle\rangle, \tag{3.4}$$

where $\vec{k}_T = \vec{k}_1 + \ldots + \vec{k}_n$, and the double brackets denote a CFT correlator on the boundary. The scalar operators $\mathcal{O}$ have scaling dimension Δ, and are dual to scalar fields ϕ in the bulk with mass

$$m^2 = \Delta(d - \Delta). \tag{3.5}$$

Note that $\Delta = d$ describes minimally coupled scalars while $\Delta = (d + 1)/2$ describes conformally coupled scalars.

The wavefunction coefficients Ψ_n satisfy conformal Ward identities (CWIs), which are a consequence of the de Sitter isometries. The conformal generators are D (dilatation), P_i (translations), K_i (special conformal transformations), and M_{ij} (rotations). The CWIs can be cast as

$$\sum_{a=1}^{n} P_a^i \Psi_n = \sum_{a=1}^{n} D_a \Psi_n = \sum_{a=1}^{n} K_a^i \Psi_n = \sum_{a=1}^{n} M_a^{ij} \Psi_n = 0, \tag{3.6}$$

where $a, b, \ldots$ are particle labels and

$$\begin{aligned}
P^i &= k^i, \\
D &= k^i \partial_i + (d - \Delta), \\
K_i &= k_i \partial^j \partial_j - 2k^j \partial_j \partial_i - 2(d - \Delta)\partial_i, \\
M_{ij} &= (k_i \partial_j - k_j \partial_i),
\end{aligned} \tag{3.7}$$

with $\partial_i = \frac{\partial}{\partial k^i}$. Observe here that the conformal dimension of the scalars appear explicitly in generators. Boundary vector indices will be freely raised and lowered here using a flat metric.

3.1 Witten diagrams

From a more traditional field theory perspective, the wavefunction coefficients can be computed through Witten diagrams [7, 10, 11].

The scalar equation of motion is given by

$$[\eta^2\partial_\eta^2 + (1-d)\eta\partial_\eta - \eta^2\partial^i\partial_i + m^2]\phi = 0. \tag{3.8}$$

We will consider momentum eigenstates, such that $\phi = \mathcal{K}_\nu(k,\eta)e^{i\vec{k}\cdot\vec{x}}$, with $\mathcal{K}_\nu(k,\eta)$ denoting the bulk-to-boundary propagator:

$$\mathcal{K}_\nu(k,\eta) = \mathcal{N}k^\nu\eta^{d/2}H_\nu(-k\eta). \tag{3.9}$$

Here, $\nu = \Delta - d/2$, $k = |\vec{k}|$, H_ν is a Hankel function of the second kind, and we will leave the normalisation $\mathcal{N}$ unspecified for now. $\mathcal{K}_\nu(k,\eta)$ satisfies $(\mathcal{D}_k^2 + m^2)\mathcal{K}_\nu = 0$, with

$$\mathcal{D}_k^2 \equiv \eta^2\partial_\eta^2 + (1-d)\eta\partial_\eta + \eta^2 k^2. \tag{3.10}$$

Contact diagrams are given by a product of bulk-to-boundary propagators integrated over the bulk, expressed as

$$\mathcal{C}_n^\Delta \equiv \int \frac{d\eta}{\eta^{d+1}}U_{1,n}(\eta), \tag{3.11}$$

$$U_{m,n}(\eta) = \prod_{a=m}^n \mathcal{K}_\nu(k_a,\eta). \tag{3.12}$$

More general Witten diagrams involve also bulk-to-bulk propagators, $G_\nu(k,\eta,\tilde{\eta})$, satisfying

$$(\mathcal{D}_k^2 + m^2)G_\nu = \eta^{d+1}\delta(\eta - \tilde{\eta}). \tag{3.13}$$

As it turns out, however, any tree level diagram can be obtained from contact diagrams through certain differential operations.

In order to see this, let us first consider the action of the boundary generators in (3.7) on bulk-to-boundary propagators. It can be expressed in terms of derivatives with respect to conformal time

$$D\mathcal{K}_\nu = \eta\frac{\partial}{\partial\eta}\mathcal{K}_\nu, \qquad P^i\mathcal{K}_\nu = k^i\mathcal{K}_\nu,$$
$$K_i\mathcal{K}_\nu = \eta^2 k_i\mathcal{K}_\nu, \quad M_{ij}\mathcal{K}_\nu = 0. \tag{3.14}$$

Now consider the following operator

$$\mathcal{D}_a \cdot \mathcal{D}_b = \frac{1}{2}(P_a^i K_{bi} + K_{ai}P_b^i - M_{a,ij}M_b^{ij}) + D_a D_b. \tag{3.15}$$

Using (3.14) one finds that

$$(\mathcal{D}_a \cdot \mathcal{D}_b)\mathcal{K}_\nu^a\mathcal{K}_\nu^b = \eta^2[\partial_\eta\mathcal{K}_\nu^a\partial_\eta\mathcal{K}_\nu^b + (\vec{k}_a \cdot \vec{k}_b)\mathcal{K}_\nu^a\mathcal{K}_\nu^b], \tag{3.16}$$

with shorthand notation $\mathcal{K}_\nu^a = \mathcal{K}_\nu(k_a,\eta)$. This observation can then be used to show that

$$(\mathcal{D}_{1...p}^2 U_{1,p})U_{p+1,n} = (\mathcal{D}_1 + \ldots + \mathcal{D}_p)^2 U_{1,n}, \tag{3.17}$$

where in the left hand side $\mathcal{D}_{1\ldots p}^2$ is defined in (3.10) with $k = |\vec{k}_1 + \ldots + \vec{k}_p| \equiv k_{1\ldots p}$ and $p < n$, and the right hand side is built using the boundary conformal generators in momentum space (3.7), satisfying $\mathcal{D}_a \cdot \mathcal{D}_a = -m^2$. In particular, we can derive the following identity,

$$[(\mathcal{D}_1 + \ldots + \mathcal{D}_p)^2 + m^2]^{-1}\mathcal{C}_n^\Delta = \int \frac{d\eta}{\eta^{d+1}}\frac{d\tilde{\eta}}{\tilde{\eta}^{d+1}}U_{p+1,n}(\eta)G_\nu(k_{1\ldots p},\eta,\tilde{\eta})U_{1,p}(\tilde{\eta}), \qquad (3.18)$$

which can be easily demonstrated using (3.17) and the equation of motion of the bulk-to-bulk propagator (3.13). Therefore, any tree level exchange diagram can be recast as a differential operator given in terms of the boundary momenta acting on a contact diagram.

Finally, observe that acting with $\mathcal{D}_a \cdot \mathcal{D}_b$ on a pair of bulk-to-boundary propagators is equivalent to acting with $\nabla_a \cdot \nabla_b$, where ∇_a is a bulk covariant derivative acting on leg a. This identity will be very useful for computing Witten diagrams for derivative interactions containing terms of the form $\nabla\phi \cdot \nabla\phi$. Another useful identity is

$$\begin{aligned}[(\mathcal{D}_a \cdot \mathcal{D}_b),(\mathcal{D}_b \cdot \mathcal{D}_c)]\mathcal{C}_n^\Delta &= 2(K_a \cdot P_c - P_a \cdot K_c)D_b\mathcal{C}_n + \text{cyc}(abc), \\ &= 0. \end{aligned} \qquad (3.19)$$

The commutator is not zero but vanishes when acting on a contact diagram. This was first derived in the embedding space formalism [34], and its generalization to momentum space is straightforward. Using (3.14) we can easily show that the right hand side vanishes.

3.2 Four-point wavefunction coefficients

Our strategy in this section will be to lift the effective actions in section 2.1 to de Sitter space up to four point interactions, use them to compute the four-point wavefunction coefficients using Witten diagrams, and express the result in terms of boundary conformal generators acting on a contact term. It will be convenient to define the following operators:

$$\hat{s} = \mathcal{D}_1 \cdot \mathcal{D}_2, \quad \hat{t} = \mathcal{D}_1 \cdot \mathcal{D}_4, \quad \hat{u} = \mathcal{D}_1 \cdot \mathcal{D}_3, \qquad (3.20)$$

which satisfy

$$\hat{s} + \hat{t} + \hat{u} = m^2, \qquad (3.21)$$

when acting on contact diagrams. This can be seen using the CWIs in (3.6).

In de Sitter space, the expansion of the NLSM action up to four points can be cast as

$$S_4^{\text{NLSM}} = -\int d^4x \sqrt{-g}\,\text{Tr}\left\{\tfrac{1}{2}\nabla\Phi \cdot \nabla\Phi + \tfrac{1}{2}m^2\Phi^2 + \lambda^2\Phi^2\nabla\Phi \cdot \nabla\Phi + \tfrac{1}{4}C\Phi^4\right\}, \qquad (3.22)$$

where we have included a mass term and a possible quartic interaction coming from a curvature correction (recall we have set the dS radius to one). The mass is also proportional to the curvature and vanishes in the flat space limit. Using the identity (3.16), it is straightforward to show that the four-point wavefunction coefficient obtained from Witten diagrams is given by

$$\Psi_4^{\text{NLSM}} = \delta^3(\vec{k}_T)\left[2\lambda^2\left(\hat{s} + \hat{t}\right) - C\right]\mathcal{C}_4^\Delta = -\delta^3(\vec{k}_T)\left(2\lambda^2\hat{u} + C\right)\mathcal{C}_4^\Delta. \qquad (3.23)$$

Up to quartic vertices and six-derivative interactions, the most general effective action for a scalar field in (A)dS is given by [73]

$$S_4^{(6)} = -\int d^4x \sqrt{-g} \left\{ \tfrac{1}{2}\nabla\phi\cdot\nabla\phi + \tfrac{1}{2}m^2\phi^2 + \tfrac{1}{8}A(\nabla_\mu\nabla_\nu\phi)^2\nabla\phi\cdot\nabla\phi + \tfrac{1}{8}B(\nabla\phi\cdot\nabla\phi)^2 + \tfrac{1}{4!}C\phi^4 \right\},$$
(3.24)

where A, B, and C are undetermined numerical coefficients. Other possible interactions are related by integration by parts or the free equation of motion $\nabla^2\phi = -m^2\phi$. For the sGal theory, the 6-derivative interaction is the naive uplift of the one in (2.3) while the lower-derivative interactions correspond to curvature corrections and a mass term. In the flat space limit, these are subleading and the action reduces to (2.3) for $A = \lambda$. Hence, (3.24) represents the uplift of the special Galileon theory to a curved background, with unfixed coefficients corresponding to curvature corrections. Additional data must be specified in order to fix them, such as soft limits, and we will explore this section 5. For the DBI theory, we set $A = 0, B = \lambda$, and there is a single curvature correction with unfixed coefficient C. In the flat space limit, the action reduces to (2.2) up to quartic interactions.

The four-point wavefunction coefficient obtained from (3.24) is

$$\Psi_4^{(6)} = \delta^3(\vec{k}_T)[A(\hat{s}^3 + \hat{t}^3 + \hat{u}^3) + (dA - B)(\hat{s}^2 + \hat{t}^2 + \hat{u}^2) - C]\mathcal{C}_4^\Delta.$$
(3.25)

We can illustrate this derivation using Witten diagrams. For example, let's consider the six-derivative interaction term

$$(\nabla_\mu\nabla_\nu\phi)^2\,\nabla\phi\cdot\nabla\phi = \eta^6\eta^{\mu\nu}\eta^{\rho\sigma}\eta^{\kappa\lambda}(\nabla_\mu\phi)(\nabla_\nu\phi)(\nabla_\rho\nabla_\kappa\phi)(\nabla_\sigma\nabla_\lambda\phi),$$
$$= \eta^6(\partial_\mu\phi\partial^\mu\phi)\eta^{\rho\sigma}\eta^{\kappa\lambda}(\partial_\rho\partial_\kappa - \Gamma^\alpha_{\rho\kappa}\partial_\alpha\phi)(\partial_\sigma\partial_\lambda\phi - \Gamma^\beta_{\sigma\lambda}\partial_\beta\phi).$$
(3.26)

The corresponding tree-level Witten diagrams are given by

$$\int_{-\infty}^0 \frac{d\eta}{\eta^4}\eta^6 \bigg[(\vec{k}_1\cdot\vec{k}_2)^2\mathcal{K}_1\mathcal{K}_2 + 2\vec{k}_1\cdot\vec{k}_2\dot{\mathcal{K}}_1\dot{\mathcal{K}}_2 + \ddot{\mathcal{K}}_1\ddot{\mathcal{K}}_2$$
$$+ \frac{1}{\eta}\left(2\vec{k}_1\cdot\vec{k}_2(\mathcal{K}_1\dot{\mathcal{K}}_2 + \dot{\mathcal{K}}_1\mathcal{K}_2) - k_1^2\mathcal{K}_1\dot{\mathcal{K}}_2 - k_2^2\dot{\mathcal{K}}_1\mathcal{K}_2 + \dot{\mathcal{K}}_1\ddot{\mathcal{K}}_2 + \ddot{\mathcal{K}}_1\dot{\mathcal{K}}_2 \right)$$
(3.27)
$$+ \frac{2}{\eta^2}\left(\vec{k}_1\cdot\vec{k}_2\mathcal{K}_1\mathcal{K}_2 + 2\dot{\mathcal{K}}_1\dot{\mathcal{K}}_2 \right) \bigg] \left[\vec{k}_3\cdot\vec{k}_4\mathcal{K}_3\mathcal{K}_4 + \dot{\mathcal{K}}_3\dot{\mathcal{K}}_4 \right] + \dots,$$

where $\mathcal{K}_a$ are bulk-to-boundary propagators, $\dot{\mathcal{K}}_a$ denotes a derivative with respect to conformal time, and the ellipsis denotes the t and u channels. If we recast this result in terms of differential operators acting on a contact diagram we see that

$$-\frac{1}{8}\left(\nabla_\mu\nabla_\nu\phi\right)^2\nabla\phi\cdot\nabla\phi \to \left[\hat{s}^3 + \hat{t}^3 + \hat{u}^3 + d\left(\hat{s}^2 + \hat{t}^2 + \hat{u}^2\right) \right]\mathcal{C}_4^\Delta.$$
(3.28)

The other terms in (3.25) can be directly derived from (3.24) using (3.16). In appendix A we evaluate a 6-point NLSM wavefunction coefficient using Witten diagrams.

4 de Sitter wavefunction coefficients from the worldsheet

In this section we will use the cosmological scattering equations introduced in [43] to compute the four-point wavefunction coefficients obtained from Witten diagrams in the previous section.

4.1 Cosmological scattering equations

In order to lift the scattering equations to de Sitter space, we replace $k_a \cdot k_b$ in (2.4) with differential operators acting in the future boundary, given by (3.15), and introduce a mass deformation. The scattering equations then have an operatorial character,

$$S_a = \sum_{\substack{b=1 \\ b \neq a}}^{n} \frac{2\left(\mathcal{D}_a \cdot \mathcal{D}_b\right) + \mu_{ab}}{\sigma_{ab}} \equiv \sum_{\substack{b=1 \\ b \neq a}}^{n} \frac{\alpha_{ab}}{\sigma_{ab}} \,, \tag{4.1}$$

where $\mu_{a\,a\pm1} = -m^2$ modulo n and zero otherwise. This mass deformation is analogous to the flat space one in [74] and assumes canonical ordering of the external legs $\mathbb{I}_n = (1, 2, \ldots, n)$. These are referred to as cosmological scattering equations (CSE). The CWIs in (3.6) can be recast as

$$\sum_{b \neq a} \alpha_{ab} \Psi_n = 0, \tag{4.2}$$

where a is any external leg and we sum over b. This implies an underlying $\mathrm{SL}(2, \mathbb{C})$ symmetry in the scattering equations, just like in flat space. This symmetry can be used to fix the location of three punctures. For more details, see [44].

The worldsheet formula in (2.5) can then be lifted to de Sitter space as follows:

$$\Psi_n = \delta^d(\vec{k}_T) \int_\gamma \prod_{a \neq b,c,d}^{n} \mathrm{d}\sigma_a \, S_a^{-1} (\sigma_{bc}\sigma_{cd}\sigma_{db})^2 \, \mathcal{I}_n \mathcal{C}_n^\Delta, \tag{4.3}$$

where the integrand may also contain boundary conformal generators. For theories with ϕ^n interactions, we are free to shuffle the CSE with other terms in the integrand $\mathcal{I}_n$ [44]. On the other hand, this may not be the case for derivative interactions, and we believe this issue calls for a more systematic investigation in the future. In this work we fix the ordering with CSE appearing to the left of the integrand.

The flat space integrands were constructed from Pfaffians defined in (2.9). Their obvious uplift to de Sitter is through the matrix

$$A_{rs} = \begin{cases} \dfrac{\alpha_{rs}}{\sigma_{rs}}, & r \neq s, \\[2mm] 0, & r = s. \end{cases} \tag{4.4}$$

As discussed previously, theories with higher-derivative interactions can have curvature corrections that are absent in flat space. Therefore, we cannot simply lift the flat space integrands in section 2.2 to dS by replacing kinematic invariants with differential operators. This procedure has to be supplemented by curvature corrections and mass deformations, which we will describe in the following subsections.

4.2 Building blocks

There are four basic building blocks for the four-point integrands. Here we will describe each of them, explaining how to evaluate the corresponding worldsheet integrals.

The simplest building block is

$$\mathcal{I}^{\phi^4} = \mathrm{PT} \, \mathrm{Pf}X|_{\mathrm{conn}} \, \mathrm{Pf}'A, \tag{4.5}$$
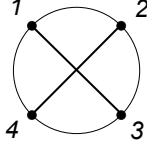
Figure 1. Graphic representation of $\mathrm{PT}\,\mathrm{Pf}X|_{\mathrm{conn}}$. The circle refers to the PT factor while the intersecting lines correspond to $\mathrm{Pf}X|_{\mathrm{conn}}$.

where the matrix X is defined in (2.13) and

$$\mathrm{Pf}\,X = \frac{1}{\sigma_{12}\sigma_{34}} - \frac{1}{\sigma_{13}\sigma_{24}} + \frac{1}{\sigma_{23}\sigma_{14}}, \tag{4.6}$$

$$\mathrm{Pf}\,X|_{\mathrm{conn}} = -\frac{1}{\sigma_{13}\sigma_{24}}. \tag{4.7}$$

The integrand (4.5) describes a contact diagram for a ϕ^4 interaction [43, 56]. Note that at four-points, $\mathrm{Pf}\,X$ can be written as a sum of three terms which correspond to perfect matchings and $\mathrm{Pf}X|_{\mathrm{conn}}$ refers to the connected perfect matching with respect to the ordering of the Parke-Taylor factor (see figure 1). Fixing legs $\{1, 2, 4\}$ and deleting legs $\{2, 4\}$ from the A-matrix in the Pfaffian leads to the wavefunction coefficient

$$\Psi_4^{\phi^4} = -\delta^3(\vec{k}_T) \int_{\gamma_3} d\sigma_3 \, (\sigma_{41}\sigma_{12}\sigma_{24})^2 \left[\frac{1}{\sigma_{12}\sigma_{23}\sigma_{34}\sigma_{41}} \frac{\sigma_{13}\sigma_{23}\sigma_{43}}{\hat{S}_3} \frac{\alpha_{13}}{(\sigma_{13}\sigma_{24})^2} \right] \mathcal{C}_4^{\Delta}, \tag{4.8}$$

where the contour γ_3 encircles the pole arising from S_3. The first term in the integrand is the standard Jacobian associated with the $\mathrm{SL}(2, \mathbb{C})$ fixing, and we have rescaled the third scattering equation to

$$\hat{S}_3 = \alpha_{13}\sigma_{23}\sigma_{43} + \alpha_{23}\sigma_{13}\sigma_{43} + \alpha_{43}\sigma_{13}\sigma_{23}. \tag{4.9}$$

After some cancellations we see there is only a simple pole at $\sigma_{13} = 0$ so we wrap the contour around this pole to obtain

$$\Psi_4^{\phi^4} = \delta^3(\vec{k}_T) \int_{\gamma_3} d\sigma_3 \left[\frac{\sigma_{41}\sigma_{12}}{\sigma_{13}} \frac{1}{\hat{S}_3} \alpha_{13} \right] \mathcal{C}_4 = -\delta^3(\vec{k}_T) \int_{\sigma_{13}} d\sigma_3 \left[\frac{\sigma_{41}\sigma_{12}}{\sigma_{13}} \frac{1}{\hat{S}_3} \alpha_{13} \right] \mathcal{C}_4^{\Delta}. \tag{4.10}$$

Computing the residue then gives

$$\Psi_4^{\phi^4} = -\delta^3(\vec{k}_T) \left[\frac{\sigma_{12}\sigma_{41}}{\hat{S}_3} \bigg|_{\sigma_{13}=0} \alpha_{13} \right] \mathcal{C}_4^{\Delta} = \delta^3(\vec{k}_T) \mathcal{C}_4^{\Delta}. \tag{4.11}$$

Next we consider the naive uplifts of the flat space integrands of section 2.2. Note that these uplifts will not describe the full four-point wavefunction coefficients in dS because they will be missing mass deformations and curvature corrections. We will explain how to encode these additional terms in the worldsheet integrands in the next subsection. The naive uplift of the NLSM integrand in (2.6) is given by

$$\mathcal{I}^{\mathrm{NLSM}} = \mathrm{PT} \left(\mathrm{Pf}'A \right)^2. \tag{4.12}$$

– 11 –

As before, we will fix legs $\{1, 2, 4\}$ and delete legs $\{2, 4\}$ from the A-matrix to obtain

$$\Psi_4^{\text{NLSM}} = \delta^3(\vec{k}_T) \int_{\gamma_3} d\sigma_3 \, (\sigma_{41}\sigma_{12}\sigma_{24})^2 \left[\frac{1}{\sigma_{12}\sigma_{23}\sigma_{34}\sigma_{41}} \frac{\sigma_{13}\sigma_{23}\sigma_{43}}{\hat{S}_3} \left(\frac{\alpha_{13}}{\sigma_{13}\sigma_{24}} \right)^2 \right] \mathcal{C}_4^\Delta . \quad (4.13)$$

After simplifying the integrand there is once again a simple pole at $\sigma_{13} = 0$, so we wrap the contour around this pole:

$$\Psi_4^{\text{NLSM}} = -\delta^3(\vec{k}_T) \int_{\gamma_3} d\sigma_3 \left[\frac{\sigma_{12}\sigma_{41}}{\sigma_{13}} \frac{1}{\hat{S}_3} \alpha_{13}^2 \right] \mathcal{C}_4^\Delta = \delta^3(\vec{k}_T) \int_{\sigma_{13}=0} d\sigma_3 \left[\frac{\sigma_{12}\sigma_{41}}{\sigma_{13}} \frac{1}{\hat{S}_3} \alpha_{13}^2 \right] \mathcal{C}_4^\Delta . \tag{4.14}$$

Evaluating the residue of this pole finally gives

$$\Psi_4^{\text{NLSM}} = \delta^3(\vec{k}_T) \left[\frac{\sigma_{12}\sigma_{41}}{\hat{S}_3} \bigg|_{\sigma_{13}=0} \alpha_{13}^2 \right] \mathcal{C}_4^\Delta = -\delta^3(\vec{k}_T) \alpha_{13} \, \mathcal{C}_4^\Delta . \tag{4.15}$$

In appendix B, we generlise this computation to 6-points. This will illustrate a number subtleties that can arise for worldsheet descriptions of theories with derivative interactions, such as the presence of higher-order poles and potential ordering ambiguities.

Now we analyse the naive uplift of the DBI integrand,

$$\mathcal{I}^{\text{DBI}} = \text{Pf}X \left(\text{Pf}'A \right)^3 . \tag{4.16}$$

Fixing legs $\{1, 2, 4\}$ as above, we find

$$\Psi_4^{\text{DBI}} = \delta^3(\vec{k}_T) \int_{\gamma_3} d\sigma_3 (\sigma_{14}\sigma_{12}\sigma_{24})^2 \left[\text{Pf}X \frac{1}{S_3} \left(\text{Pf}'A \right)^3 \right] \mathcal{C}_4^\Delta . \tag{4.17}$$

Recall from (4.6) that $\text{Pf}X$ has three terms. To evaluate the worldsheet integral containing the first term, it is convenient to choose $(\text{Pf}'A)^3 = (\text{Pf}A_{23}^{23})^2(\text{Pf}A_{24}^{24})$ such that

$$\Psi_4^{12,34} = \delta^3(\vec{k}_T) \int_{\gamma_3} d\sigma_3 \frac{(\sigma_{14}\sigma_{12}\sigma_{24})^2}{\sigma_{12}\sigma_{34}} \left[\frac{\sigma_{13}\sigma_{23}\sigma_{43}}{\hat{S}_3} \left(\frac{\alpha_{14}}{\sigma_{14}\sigma_{23}} \right)^2 \frac{\alpha_{13}}{\sigma_{13}\sigma_{24}} \right] \mathcal{C}_4^\Delta , \tag{4.18}$$

where the superscript on Ψ_4 denotes the contribution from the first term in (4.6). The contour integral can be evaluated as above to obtain

$$\Psi_4^{12,34} = \delta^3(\vec{k}_T) \left[\frac{\sigma_{12}\sigma_{24}}{\hat{S}_3} \bigg|_{\sigma_{23}=0} \alpha_{14}^2 \alpha_{13} \right] \mathcal{C}_4^\Delta = -\delta^3(\vec{k}_T) \alpha_{14}\alpha_{13} \mathcal{C}_4^\Delta , \tag{4.19}$$

where we wrapped the contour around the pole $\sigma_{23} = 0$, evaluated the residue, and used the CWI to cancel α_{23} in the denominator with α_{14} in the numerator. Note that the ordering of α_{14} and α_{13} in the final result is not important due to (3.19). For the remaining two terms in (4.17) we choose $(\text{Pf}'A)^3$ to be $(\text{Pf}A_{14}^{14})^2(\text{Pf}A_{12}^{12})$ and $(\text{Pf}A_{13}^{13})^2(\text{Pf}A_{12}^{12})$, respectively. Using similar manipulations, we finally obtain

$$\Psi_4^{\text{DBI}} = -\delta^3(\vec{k}_T) \left(\alpha_{12}\alpha_{14} + \alpha_{14}\alpha_{13} + \alpha_{13}\alpha_{12} \right) \mathcal{C}_4^\Delta . \tag{4.20}$$

This choice of Pfaffians avoids higher-order poles in the worldsheet coordinates which are more subtle to evaluate. We describe such an example in appendix C. It will also be useful to consider the following integrand, whose corresponding wavefunction coefficient follows trivially from the above calculation:

$$(\mathrm{Pf}'A)^3 \, \mathrm{Pf}X|_{\mathrm{conn}} \to -\delta^3(\vec{k}_T)\alpha_{12}\alpha_{14}\mathcal{C}_4^\Delta. \tag{4.21}$$

Finally, let us consider the naive uplift of the special Galileon integrand

$$\mathcal{I}^{\mathrm{sGal}} = \left(\mathrm{Pf}'A\right)^4. \tag{4.22}$$

In this case, the four-point wavefunction coefficient is given by

$$\Psi_4^{\mathrm{sGal}} = \delta^3(\vec{k}_T) \int_{\gamma_3} d\sigma_3 \, (\sigma_{14}\sigma_{12}\sigma_{24})^2 \left[\frac{1}{S_3}\left(\mathrm{Pf}'A\right)^4\right] \mathcal{C}_4^\Delta. \tag{4.23}$$

As in the DBI case, there are Pfaffian choices exclusively leading to simple poles. The following choice leads to a permutation invariant result:

$$(\mathrm{Pf}'A)^4 = \frac{1}{3}\left\{\frac{1}{\sigma_{34}^2}(\mathrm{Pf}A_{34}^{34})^2 \frac{(-1)}{\sigma_{23}}(\mathrm{Pf}A_{23}^{23})\frac{1}{\sigma_{24}}\left(\mathrm{Pf}A_{24}^{24}\right) + \mathrm{cyclic}(2,3,4)\right\}. \tag{4.24}$$

Note that other choices can give different results due to non-trivial commutators which only vanish in the flat space limit. Hence we must specify a choice of Pfaffian. Following closely the computations above, we obtain

$$\Psi_4^{\mathrm{sGal}} = \frac{1}{3}\delta^3(\vec{k}_T)\left(\alpha_{12}\alpha_{14}\alpha_{13} + \alpha_{14}\alpha_{13}\alpha_{12} + \alpha_{13}\alpha_{14}\alpha_{12}\right)\mathcal{C}_4^\Delta. \tag{4.25}$$

Using (3.19), it is not difficult to see that the above expression is permutation invariant.

4.3 Generalised double copy

Using the building blocks in the previous subsection (in particular (4.11) and (4.15)), we see that the four-point NLSM wavefunction coefficient (including a curvature correction) in (3.23) follows from the following integrand:

$$\mathcal{I}_4^{\mathrm{NLSM}} = \lambda^2 \mathrm{PT}\left(\mathrm{Pf}'A\right)^2 + c\mathrm{PT}\,\mathrm{Pf}X|_{\mathrm{conn}}\mathrm{Pf}'A, \tag{4.26}$$

if we identify the unfixed parameter c with $-C$. Now consider the following shift of the first term in (4.26):

$$\lambda^2 \mathrm{PT} \to a\mathrm{Pf}'A\left(\mathrm{Pf}'A + m^2\,\mathrm{Pf}X|_{\mathrm{conn}}\right) + b\left(\mathrm{Pf}'A\mathrm{Pf}X + m^2\mathrm{PT}\right), \tag{4.27}$$

where a and b are also free coefficients. We then obtain the following integrand:

$$\mathcal{I}_4^{(6)} = a(\mathrm{Pf}'A)^3(\mathrm{Pf}'A + m^2\,\mathrm{Pf}X|_{\mathrm{conn}}) + b(\mathrm{Pf}'A)^2(\mathrm{Pf}'A\mathrm{Pf}X + m^2\mathrm{PT}) + c\mathrm{PT}\,\mathrm{Pf}X|_{\mathrm{conn}}\mathrm{Pf}'A. \tag{4.28}$$

Using the prescription for evaluating worldsheet integrals described the previous subsection (in particular (4.11), (4.15), (4.20), (4.21), and (4.25)), we see that the corresponding wavefunction coefficient is

$$\Psi_4^{(6)} = \delta^3(\vec{k}_T) \left[\tfrac{8}{3} a(\tilde{s}\tilde{t}\tilde{u} + \tilde{t}\tilde{u}\tilde{s} + \tilde{u}\tilde{s}\tilde{t}) - 4b(\tilde{s}\tilde{t} + \tilde{t}\tilde{u} + \tilde{u}\tilde{s}) + c \right] \mathcal{C}_4^\Delta, \qquad (4.29)$$

where $\tilde{s}$, $\tilde{t}$, and $\tilde{u}$ are related to their hatted counterparts (3.20) as

$$\tilde{s} = \hat{s} - \tfrac{1}{2}m^2, \quad \tilde{t} = \hat{t} - \tfrac{1}{2}m^2, \quad \tilde{u} = \hat{u} - \tfrac{1}{2}m^2. \qquad (4.30)$$

It is then straightforward to match (4.29) with (3.25) via the following identification of unfixed coefficients:

$$A = \tfrac{8}{3}a, \quad B = 2a\left(m^2 + \tfrac{4}{3}d\right) - 2b, \quad C = -\tfrac{1}{3}am^6 + bm^4 - c. \qquad (4.31)$$

Hence, the worldsheet integrand (4.28) encodes the effective action in (3.24). Moreover, (4.27) can be thought of as a double copy procedure encoding mass deformations and curvature corrections. In particular, it reduces to (2.16) and (2.15) in the flat space limit for $a \neq 0$ and $a = 0$, respectively (recalling that the mass is measured in units of the inverse dS radius). We therefore refer to this as a generalised double copy. Note that this prescription leaves the curvature corrections and mass deformations unfixed. To fix these coefficients, we must specify additional data beyond the flat space limit. We will suggest a strategy for doing this in the next section.

5 Soft limits

In the previous section, we found the building blocks of four-point wavefunction coefficients of scalar EFTs in dS to be:

$$\mathcal{C}_4^\Delta, \quad \hat{u}\mathcal{C}_4^\Delta, \quad \left(\hat{s}^2 + \hat{t}^2 + \hat{u}^2\right)\mathcal{C}_4^\Delta, \quad \left(\hat{s}^3 + \hat{t}^3 + \hat{u}^3\right)\mathcal{C}_4^\Delta. \qquad (5.1)$$

For notational simplicity, we will leave out the delta function imposing momentum conservation along the boundary. The first one is a ϕ^4 contact diagram, while the remaining building blocks arise from the action on this contact diagram with the differential operators defined in (3.20). The first two terms contribute when lifting NLSM to dS, while the last two arise when lifting the DBI and sGal theories. In this section, we will compute these objects explicitly in the cases $\Delta = 2, 3$ and analyse their soft limits. In practice, all the integrals we encounter will be of the form $\int_{-\infty}^0 \eta^\alpha e^{-iE\eta} d\eta$. To evaluate them, we rotate the contour clockwise onto the complex plane so that the integrand is exponentially damped as $\eta \to -\infty$ [10]. To simplify our expressions we will set the normalisation of the bulk-to-boundary propagators in (3.9) to be $\mathcal{N} = (-1)^{\nu - \frac{1}{2}} \sqrt{2/\pi}$.

We will show that the soft limits of the building blocks in (5.1) are given in terms of boundary conformal generators acting on certain three-point contact diagrams. Soft limits play an important role in cosmology where they appear in constraints relating higher-point functions to symmetry transformations of lower-point functions [7, 75–77] and allow one

to deduce 3-point inflationary correlators from four-point dS correlators [16, 78–81]. Soft limits of DBI and sGal wavefunction coefficients in flat space were recently analysed in [67]. Note that the soft limit of the four-point wavefunction coefficients in (3.23) and (3.25) can be obtained from linear combinations of soft limits we derive in this section. By appropriately choosing the coefficients of curvature corrections in the corresponding EFTs in (3.22) and (3.24) we can set many of these terms to zero, which may signal the existence of hidden symmetries.

5.1 Contact diagram

Let us first consider the four-point contact diagram. For conformally coupled scalars, we find

$$\mathcal{C}_4^{\Delta=2} = \int \frac{d\eta}{\eta^4} \left(\prod_{i=1}^4 \mathcal{K}_{1/2}^i \right) = \frac{1}{E}. \tag{5.2}$$

It is trivial to see that the soft limit of this quantity corresponds to a three-point contact diagram for conformally coupled scalars with a time-dependent interaction:

$$\lim_{\vec{k}_1 \to 0} C_4^{\Delta=2} = \mathcal{C}_{3,\eta}^{\Delta=2}, \tag{5.3}$$

where

$$\mathcal{C}_{3,\eta}^{\Delta=2} = \int \frac{d\eta}{\eta^4} \left(\eta \prod_{i=2}^4 \mathcal{K}_{1/2}^i \right) = \frac{1}{E}. \tag{5.4}$$

This three-point contact diagram will also arise in the soft limit of more complicated four-point wavefunction coefficients of conformally coupled scalars. In particular, we will obtain conformal generators acting on (5.4).

For minimally coupled scalars, the integrals need to be regulated. We will use the prescription $d \to d + 2\epsilon$, $\Delta \to \Delta + \epsilon$, which leaves the spectral parameter $\nu = \Delta - d/2$ unchanged [82–85], such that

$$\begin{aligned}
\mathcal{C}_4^{\Delta=3+\epsilon} &= \int \frac{d\eta}{\eta^{4+2\epsilon}} \prod_{i=1}^4 \mathcal{K}_{3/2}^i, \\
&= \frac{1}{E^{2\epsilon}} \bigg\{ E^3 [\Gamma(-2+2\epsilon) + \Gamma(-3+2\epsilon)] + \Gamma(2\epsilon)(k_1 k_2 k_3 + \ldots) \\
&\qquad + \Gamma(-1+2\epsilon) E (k_1 k_2 + \ldots) + \frac{k_1 k_2 k_3 k_4}{E} \Gamma(1+2\epsilon) \bigg\},
\end{aligned} \tag{5.5}$$

where the ellipsis inside each parenthesis denotes all permutations involving the four legs. We then find the following soft limit:

$$\begin{aligned}
\lim_{\vec{k}_1 \to 0} \mathcal{C}_4^{\Delta=3+\epsilon} = \frac{1}{E^{2\epsilon}} \{ &E^3 [\Gamma(-2+2\epsilon) + \Gamma(-3+2\epsilon)] + \Gamma(2\epsilon) k_2 k_3 k_4 \\
&+ \Gamma(-1+2\epsilon) E(k_2 k_3 + k_2 k_4 + k_3 k_4) \}.
\end{aligned} \tag{5.6}$$

We can now compare this with the three-point contact diagram of minimally coupled scalars:

$$\mathcal{C}_3^{\Delta=3+\epsilon} = \int \frac{d\eta}{\eta^{4+2\epsilon}} \prod_{i=2}^4 \mathcal{K}_{3/2}^i. \tag{5.7}$$

– 15 –

Unlike the contact diagram in (5.4), this contact diagram does not contain a time-dependent interaction. After performing the integral in (5.7) and changing $\epsilon \to 2\epsilon$, we finally obtain (5.6):

$$\lim_{\vec{k}_1 \to 0} C_4^{\Delta=3+\epsilon} = \mathcal{C}_3^{\Delta=3+2\epsilon}, \tag{5.8}$$

which, for clarity, can be easily expanded in ϵ:

$$\mathcal{C}_3^{\Delta=3+\epsilon} = \frac{k_2^3 + k_3^3 + k_4^3}{3} \left(\frac{1}{\epsilon} - \gamma_E - \ln E + 1 \right) + \frac{1}{9} E^3 - k_2 k_3 k_4 + \mathcal{O}(\epsilon), \tag{5.9}$$

where γ_E is the Euler-Mascheroni constant. As we will see, (5.7) will continue to play a role in the soft limit of more complicated four-point wavefunction coefficients of minimally coupled scalars.

5.2 Two derivatives

Next, we will analyse the soft limit of $\hat{u}\mathcal{C}_4^{\Delta}$. In the conformally coupled case, it can be cast as

$$\hat{u}\mathcal{C}_4^{\Delta=2} = -\frac{2}{E^3}[\vec{k}_1 \cdot \vec{k}_3 - k_1 k_3 - \tfrac{E}{2}(k_2 + k_4)], \tag{5.10}$$

with soft limit

$$\lim_{\vec{k}_1 \to 0} \hat{u}\mathcal{C}_4^{\Delta=2} = \frac{1}{E} - \frac{k_3}{E^2}. \tag{5.11}$$

We recognise this expression as the dilatation operation:

$$D_3 \left(\frac{1}{E} \right) = \frac{1}{E} - \frac{k_3}{E^2}. \tag{5.12}$$

Hence, we find that the soft limit of (5.10) can be obtained by acting with a dilatation on the three-point contact diagram of (5.4):

$$\lim_{\vec{k}_1 \to 0} \hat{u}\mathcal{C}_4^{\Delta=2} = D_3 \, \mathcal{C}_{3,\eta}^{\Delta=2}. \tag{5.13}$$

In the minimally coupled case, we find

$$\begin{aligned}
\hat{u}\mathcal{C}_4^{\Delta=3} = \frac{\vec{k}_1 \cdot \vec{k}_3}{E} &\left[-E^2 + \sum_{i<j} k_i k_j + \frac{k_1 k_2 k_3 k_4}{E} \left(\frac{1}{k_1} + \frac{1}{k_2} + \frac{1}{k_3} + \frac{1}{k_4} + \frac{2}{E} \right) \right] \\
&- 2\frac{k_1^2 k_3^2}{E} \left(1 + \frac{k_2 + k_4}{E} + \frac{2k_2 k_4}{E^2} \right),
\end{aligned} \tag{5.14}$$

where requires dimensional regularisation in intermediate steps but has a finite output. Taking the soft limit then gives

$$\lim_{\vec{k}_1 \to 0} \hat{u}\mathcal{C}_4^{\Delta=3} = \frac{\vec{k}_1 \cdot \vec{k}_3}{E} \left(k_2^2 + k_3^2 + k_4^2 + k_2 k_3 + k_3 k_4 + k_4 k_2 - \frac{k_2 k_3 k_4}{E} \right), \tag{5.15}$$

which can be obtained by acting with a conformal boost on the three-point contact diagram in (5.7):

$$\lim_{\vec{k}_1 \to 0} \hat{u}\mathcal{C}_4^{\Delta=3} = (\vec{k}_1 \cdot \vec{K}_3) \, \mathcal{C}_3^{\Delta=3}. \tag{5.16}$$

Note that the divergences in (5.9) are removed by the action of conformal generators so we set $\epsilon = 0$. This will continue to hold for higher-derivative wavefunction coefficients so we will set $\epsilon = 0$ in those cases as well.

5.3 Four derivatives

We now consider the term $(\hat{s}^2 + \hat{t}^2 + \hat{u}^2)\mathcal{C}_4^\Delta$. For conformally coupled scalars, we obtain

$$(\hat{s}^2 + \hat{t}^2 + \hat{u}^2)\mathcal{C}_4^{\Delta=2} = \frac{24}{E^5}[(\vec{k}_1 \cdot \vec{k}_2 - k_1 k_2)(\vec{k}_3 \cdot \vec{k}_4 - k_3 k_4) + \text{cyc}(234)] - \frac{8}{E^3}\sum_{i<j} k_i k_j + \frac{4}{E}. \quad (5.17)$$

In this case the soft limit is simply

$$\lim_{\vec{k}_1 \to 0}(\hat{s}^2 + \hat{t}^2 + \hat{u}^2)\mathcal{C}_4^{\Delta=2} = \frac{4}{E^3}(k_2^2 + k_3^2 + k_4^2), \quad (5.18)$$

which can be recast as a second order combination of dilatation operators acting on the three-point contact diagram of (5.4):

$$\lim_{\vec{k}_1 \to 0}(\hat{s}^2 + \hat{t}^2 + \hat{u}^2)\mathcal{C}_4^{\Delta=2} = 2(D_2^2 + D_3^2 + D_4^2)\mathcal{C}_{3,\eta}^{\Delta=2}. \quad (5.19)$$

In the minimally coupled case, we obtain

$$\begin{aligned}
&(\hat{s}^2 + \hat{t}^2 + \hat{u}^2)\mathcal{C}_4^{\Delta=3}\\
&= \frac{24 k_1 k_2 k_3 k_4}{E^5}(\vec{k}_1 \cdot \vec{k}_2 - k_1 k_2)(\vec{k}_3 \cdot \vec{k}_4 - k_3 k_4)\\
&\quad + \frac{2}{E^3}(\vec{k}_1 \cdot \vec{k}_2)(\vec{k}_3 \cdot \vec{k}_4)\left(E^2 + E\sum_{i<j} k_i k_j + \sum_{i<j<l} k_i k_j k_l\right)\\
&\quad - \frac{2}{E^4}\left[(\vec{k}_1 \cdot \vec{k}_2)k_3^2 k_4^2(E + 2(k_1 + k_2)) + (\vec{k}_3 \cdot \vec{k}_4)k_1^2 k_2^2(E + 2(k_3 + k_4)) + \text{cyc}(234)\right].
\end{aligned} \quad (5.20)$$

We then find that the soft limit is given by

$$\begin{aligned}
\lim_{\vec{k}_1 \to 0}(\hat{s}^2 + \hat{t}^2 + \hat{u}^2)\mathcal{C}_4^{\Delta=3} = \frac{\vec{k}_1 \cdot \vec{k}_2}{E^3}\big[&4k_2^2 k_3 k_4 + k_2 E(k_3 k_4 + 2k_2(k_3 + k_4))\\
&+ E^2(2k_2^2 + k_2 k_3 + k_3 k_4 + k_4 k_2) - E^4)\big] + \text{cyc}(234),
\end{aligned} \quad (5.21)$$

which corresponds to applying the following quadratic combination of conformal generators to a three-point contact diagram:

$$\lim_{\vec{k}_1 \to 0}(\hat{s}^2 + \hat{t}^2 + \hat{u}^2)\mathcal{C}_4^{\Delta=3} = -2\big[D_2(\vec{k}_1 \cdot K_2) + \text{cyc}(234)\big]\mathcal{C}_3^{\Delta=3}. \quad (5.22)$$

In practice, the soft limits in (5.19) and (5.22) are most easily derived at the level of the integrand. In particular, this requires taking the soft limit of bulk-to-boundary propagators and their derivatives, and then using equations of motion to remove derivatives acting on the bulk-to-boundary propagator for the soft leg as well as factors of k_a^2. For example, in the conformally coupled case we have

$$\begin{aligned}
\lim_{\vec{k}_1 \to 0}(\hat{s}^2 + \hat{t}^2 + \hat{u}^2)\mathcal{C}_4^{\Delta=2} &= \int d\eta \left(\frac{1}{\eta}(-k_2^2 \dot{\mathcal{K}}_1 \mathcal{K}_2 + \dot{\mathcal{K}}_1 \ddot{\mathcal{K}}_2) - \frac{1}{\eta^2}\dot{\mathcal{K}}_1 \dot{\mathcal{K}}_2\right)\mathcal{K}_3 \mathcal{K}_4 + \text{cyc}(234),\\
&= \int \frac{d\eta}{\eta^3}[2\eta^2 \ddot{\mathcal{K}}_2 - \eta \dot{\mathcal{K}}_2 - 2\mathcal{K}_2]\mathcal{K}_3 \mathcal{K}_4 + \text{cyc}(234),\\
&= 2\left(D_2^2 + D_3^2 + D_4^2\right)\int \frac{d\eta}{\eta^3}\mathcal{K}_2 \mathcal{K}_3 \mathcal{K}_4. \quad (5.23)
\end{aligned}$$

The analogous construction in the minimally coupled case is given by

$$\lim_{\vec{k}_1 \to 0} \left(\hat{s}^2 + \hat{t}^2 + \hat{u}^2\right) \mathcal{C}_4^{\Delta=3} = (\vec{k}_1 \cdot \vec{k}_2) \int d\eta \left(\frac{2}{\eta} \mathcal{K}_1 \dot{\mathcal{K}}_2 + \frac{1}{\eta^2} \mathcal{K}_1 \mathcal{K}_2\right) \mathcal{K}_3 \mathcal{K}_4 + \text{cyc}(234),$$

$$= -2[D_2(\vec{k}_1 \cdot K_2) + \text{cyc}(234)] \int \frac{d\eta}{\eta^4} \mathcal{K}_2 \mathcal{K}_3 \mathcal{K}_4. \tag{5.24}$$

Using this method, one can also derive the soft limits in (5.13) and (5.16).

5.4 Six derivatives

Finally we consider the six derivative interaction $(\hat{s}^3 + \hat{t}^3 + \hat{u}^3)\mathcal{C}_4^{\Delta}$. In the conformally coupled case we obtain

$$(\hat{s}^3 + \hat{t}^3 + \hat{u}^3)\mathcal{C}_4^{\Delta=2}$$

$$= \left\{ \frac{90}{E^7}[(\vec{k}_1 \cdot \vec{k}_2) + (\vec{k}_3 \cdot \vec{k}_4) - k_1 k_2 - k_3 k_4]^3 + \frac{156}{E^5}[(\vec{k}_1 \cdot \vec{k}_2) - k_1 k_2][(\vec{k}_3 \cdot \vec{k}_4) - k_3 k_4] \right.$$

$$\left. - \frac{54}{E^5}(k_1 k_2 + k_3 k_4)[(\vec{k}_1 \cdot \vec{k}_2) + (\vec{k}_3 \cdot \vec{k}_4) - k_1 k_2 - k_3 k_4] - \frac{79}{E^3}(k_1 k_2 + k_3 k_4) + \text{cyc}(234) \right\} + \frac{93}{4E}, \tag{5.25}$$

with soft limit

$$\lim_{\vec{k}_1 \to 0} (\hat{s}^3 + \hat{t}^3 + \hat{u}^3)\mathcal{C}_4^{\Delta=2} = -\frac{108}{E^4} k_2 k_3 k_4 + \frac{52}{E^3}(k_2 k_3 + k_3 k_4 + k_4 k_2) - \frac{12}{E}. \tag{5.26}$$

Using the methods described above, we can obtain this by acting with the following combination of conformal generators on a three-point contact diagram:

$$\lim_{\vec{k}_1 \to 0} (\hat{s}^3 + \hat{t}^3 + \hat{u}^3)\mathcal{C}_4^{\Delta=2} = \left(6(D_2^3 + D_3^3 + D_4^3) - 22(D_2^2 + D_3^2 + D_4^2) + 20\right) \mathcal{C}_{3,\eta}^{\Delta=2}. \tag{5.27}$$

In the minimally coupled case, the expression for the integrated wavefunction coefficient can be found in appendix D. The soft limit is given by

$$\lim_{\vec{k}_1 \to 0} (\hat{s}^3 + \hat{t}^3 + \hat{u}^3)\mathcal{C}_4^{\Delta=3}$$

$$= \frac{(\vec{k}_1 \cdot \vec{k}_2)}{E^4} \big[3k_2^5 + 12k_2^4(k_3 + k_4) + k_2^3(k_3^2 + 36k_3 k_4 + k_4^2)$$

$$- k_2^2(k_3 + k_4)(11k_3^2 + 21k_3 k_4 + 11k_4^2) - 4k_2(k_3 + k_4)^2(k_3^2 + k_3 k_4 + k_4^2)$$

$$- (k_3 + k_4)^3(k_3^2 + k_3 k_4 + k_4^2) \big] + \text{cyc}(234). \tag{5.28}$$

This expression can also be recast in terms of conformal generators acting on a three-point contact diagram. For example, we can write

$$\lim_{\vec{k}_1 \to 0} (\hat{s}^3 + \hat{t}^3 + \hat{u}^3)\mathcal{C}_4^{\Delta=3} = [2(3D_2^2 - 11D_2)(\vec{k}_1 \cdot K_2) + \text{cyc}(234)]\mathcal{C}_3^{\Delta=3}. \tag{5.29}$$

Observe that these expressions are not unique. For example, the operators K_2 and D_2 do not commute and so we could choose to order them differently and pick up different

coefficients. Note also that unlike (5.27), the term in brackets in (5.29) contains no constant term. This comes from the different behavior of the soft limits for different values of Δ. The constant term in (5.27) arises from $D_2 + D_3 + D_4$ and the equivalent term in the case of massless scalars would be a sum over $\vec{k}_1 \cdot K_i$. We can rewrite this using CWI to get a contribution of order k_1^2 which we then drop as it is subleading.

Let us close this section with some general comments. Overall, we find that soft limits require both special conformal and dilatation operators acting on a contact diagram. In the conformally coupled case, it is always possible to express them exclusively in terms of dilatation operators but at the level of the integrand this is not the whole story. When considering how the integrand behaves in the soft limit we find that both types of conformal generators appear. Another interesting point is that we can obtain particularly simple soft limits by tuning coefficients in the effective action in (3.24). For example, if we choose the mass to be that of a conformally coupled scalar and set the coefficients $\{A, B, C\} = \lambda \{1, -8, -20\}$, then the soft limit of the corresponding four-point wavefunction coefficient in (3.25) is simply given by

$$\lim_{\vec{k}_1 \to 0} \Psi_4^{(6)} = 6\lambda(D_2^3 + D_3^3 + D_4^3)\mathcal{C}_{3,\eta}^{\Delta=2}. \tag{5.30}$$

It would be interesting to look for possible hidden symmetries in the corresponding EFT. We could perform a similar set of steps for $\Delta = 3$, but in this case there is an ambiguity in how to fix the coefficients since the commutators between the operators D_i and K_i are given by lower order contributions so different orderings might lead to different preferred choices for $\{A, B, C\}$.

6 Conclusion

The study of correlation functions in (Anti) de Sitter space using curved-space analogues of the scattering equations is still an ongoing endeavour. Prior to this paper, they have only been formulated for scalar theories with polynomial interactions, notably ϕ^3 [59, 60] and ϕ^4 [43, 44]. We have now initiated the study of scalar theories with derivative interactions using this framework. In particular, we study the wave function coefficients of the NLSM, DBI, and sGal theories in dS using the cosmological scattering equations. These effective scalar theories are of particular interest in flat space since their scattering amplitudes have a very elegant description and are related to each other in a simple way in terms of CHY formulae [56].

In this paper we have proposed new formulae for four-point wavefunction coefficients of different scalar EFTs in the form of worldsheet integrals which encode both curvature corrections and mass deformations. We showed that the DBI and sGal integrands can be obtained from the NLSM integrand by replacing a Parke-Taylor factor with a linear combination of simple building blocks involving Pfaffians of certain operatorial matrices. Because the integrands are constructed from differential operators which do not generally commute, this leads to potential ordering ambiguities that are absent in theories with polynomial interactions. Such ambiguities can occur in the DBI and sGal theories at four

points and the NLSM at six points. At four points we introduced a simple prescription for defining the worldsheet integrals such that the final results are permutation-invariant. We have also studied the soft limits of the resulting four-point wavefunction coefficients and derived formulae in the form of differential operators acting on three-point contact diagrams. For conformally coupled scalars, the three-point contact diagrams involve a time-dependent interaction, while for minimally coupled scalars the contact diagram is divergent and needs to be regulated. However, all divergences cancel out after acting with the appropriate combinations of boundary conformal generators.

There are a number of directions for future investigation. For example, it would be of interest to generalise our formulae to any number of points. In order to do so, there are several technical questions that need to be addressed. First of all, we need to develop a systematic classification of higher-derivative corrections to scalar EFTs analogous to the one in [73] beyond four-points, which to our knowledge has not been carried out yet. It would then be interesting to see if there is a simple generalisation of the double copy prescription in (4.27) which encodes such corrections at higher points. Secondly, we need a systematic understanding of ordering ambiguities that could arise in the corresponding worldsheet integrals and a prescription for removing them. A natural starting point along these lines would be to analyse potential ordering ambiguities in the six-point NLSM calculation in appendix B.

It would also be of great interest to apply our approach for computing wavefunction coefficients to the EFTs recently constructed in de Sitter space based on hidden symmetries [66]. Note that the effective actions we consider in this paper have general massess and curvature corrections up to four-points, so the actions derived in [66] should correspond to a particular choice of these parameters. It would then be interesting to compute the corresponding four-point wavefunction coefficients and their soft limits in terms of the building blocks derived in this paper and investigate the interplay of hidden symmetries with soft limits. Note that our double copy prescription does not fix massess or coefficients of curvature corrections, but these can be constrained by imposing simplicity of the soft limits, as we illustrate in the end of section 5. It would also be interesting to relate our results to those recently obtained in flat space [67] using the methods recently developed in [22].

Finally, it is important to extend the techniques of this paper to more realistic models by considering different worldsheet integrands encoding more general interactions and the breaking of conformal symmetry by inflation [86–88]. Moreover inflationary three-point correlators can be obtained by giving a small mass to one of the legs of a four-point function in de Sitter space (proportional to the slow-roll parameter) and then taking a soft limit [16, 78–81]. Our results in section 5 should be useful in this regard.

Acknowledgments

Figure 2. Witten diagrams for the six-point NLSM amplitude. The exchange diagram is summed over the three inequivalent cyclic permutations.

Figure 3. Four-point vertex appearing on the left-hand-side of a 6-point NLSM exchange diagram.

A Six-point NLSM wavefunction coefficients from Witten diagrams

In this appendix we extend the calculations in section 3.2 to six-points for the NLSM. At this level, we have the following Lagrangian,

$$
\mathcal{L}_{\text{NLSM}}^{\text{6-pt}} = \text{Tr} \left[-\frac{1}{2} \partial \Phi \cdot \partial \Phi - \frac{1}{2} m^2 \Phi^2 - \lambda^2 \Phi^2 \partial_\mu \Phi \partial^\mu \Phi - \frac{1}{4} C \Phi^4 \right.
$$
$$
\left. -\lambda^4 \left(\Phi^4 \partial_\mu \Phi \partial^\mu \Phi + \frac{1}{2} \Phi^2 \partial_\mu \Phi \Phi^2 \partial^\mu \Phi \right) - \frac{1}{6} F \Phi^6 \right],
$$

(A.1)

where m is the mass, and C and F are free coefficients coming from possible curvature corrections. For simplicity, we will set $m = C = F = 0$. We will write the result in terms of the boundary differential operators in (3.15) acting on a contact diagram, which we will compare against the results of a worldsheet calculation in appendix B. The final result will be free of ambiguities since all the differential operators which appear commute. A similar formula was previously derived in [34] using AdS embedding coordinates.

The wavefunction coefficient is given by a sum of exchange and contact diagrams shown in figure 2. To obtain the desired form, we must write the four-point vertices in the exchange diagrams in such a way that derivatives only act on bulk-to-boundary propagators. Let us consider the four-point vertex appearing on the left-hand-side of an exchange diagram, illustrated in figure 3. Using the Feynman rules derived from (A.1) and the identity in (3.16) we find

$$
\mathcal{A}_L = \int \frac{d\eta}{\eta^{d+1}} \eta^2 \{ \mathcal{K}_1 \mathcal{K}_2 \mathcal{K}_3 \mathcal{K}_L [(\vec{k}_1 \cdot \vec{k}_2) + (\vec{k}_2 \cdot \vec{k}_3) + (\vec{k}_3 \cdot \vec{k}_L) + (\vec{k}_L \cdot \vec{k}_1)]
$$
$$
+ \dot{\mathcal{K}}_1 \dot{\mathcal{K}}_2 \mathcal{K}_3 \mathcal{K}_L + \mathcal{K}_1 \dot{\mathcal{K}}_2 \dot{\mathcal{K}}_3 \mathcal{K}_L + \mathcal{K}_1 \mathcal{K}_2 \dot{\mathcal{K}}_3 \dot{\mathcal{K}}_L + \dot{\mathcal{K}}_1 \mathcal{K}_2 \mathcal{K}_3 \dot{\mathcal{K}}_L \},
$$

(A.2)

where $\mathcal{K}_L$ is associated to the bulk-to-bulk propagator and $\dot{\mathcal{K}} = \partial_\eta \mathcal{K}$. Using integration by parts to remove the derivatives acting on $\mathcal{K}_L$ gives

$$
\mathcal{A}_L = \int \frac{d\eta}{\eta^{d-1}} \mathcal{K}_L \Big[- 2\vec{k}_1 \cdot \vec{k}_3 \mathcal{K}_1 \mathcal{K}_2 \mathcal{K}_3 - 2\dot{\mathcal{K}}_1 \mathcal{K}_2 \dot{\mathcal{K}}_3 - k_1^2 \mathcal{K}_1 \mathcal{K}_2 \mathcal{K}_3 - k_3^2 \mathcal{K}_1 \mathcal{K}_2 \mathcal{K}_3
$$
$$
- \mathcal{K}_1 \mathcal{K}_2 \ddot{\mathcal{K}}_3 - \ddot{\mathcal{K}}_1 \mathcal{K}_2 \mathcal{K}_3 + \frac{1-d}{\eta} \left(\dot{\mathcal{K}}_1 \mathcal{K}_2 \mathcal{K}_3 + \mathcal{K}_1 \mathcal{K}_2 \dot{\mathcal{K}}_3 \right) \Big], \tag{A.3}
$$

where we have also used momentum conservation at the vertex, such that $\vec{k}_L = -(\vec{k}_1 + \vec{k}_2 + \vec{k}_3)$. Using the equations of motion for $\mathcal{K}_1$ and $\mathcal{K}_3$, we are left with

$$
\mathcal{A}_L = -2 \int \frac{dz}{z^{d+1}} \left[\mathcal{K}_2 \mathcal{K}_L \eta^2 \left(\vec{k}_1 \cdot \vec{k}_3 \mathcal{K}_1 \mathcal{K}_2 \mathcal{K}_3 + \dot{\mathcal{K}}_1 \mathcal{K}_2 \dot{\mathcal{K}}_3 \right) \right]. \tag{A.4}
$$

Performing similar manipulations on the other four-point vertices, we finally obtain

$$
\Psi_6^{\mathrm{NLSM}} = \lambda^4 \delta^3(\vec{k}_T) \left[(\alpha_{13} \alpha_{123}^{-1} \alpha_{46} - \alpha_{24}) + \mathrm{cyc}(i \to i{+}2) \right] \mathcal{C}_6^\Delta \tag{A.5}
$$

where $\alpha_{ijk} = (\mathcal{D}_i + \mathcal{D}_j + \mathcal{D}_k)^2$. Note that the first term comes from the exchange diagrams and the second term is from the contact diagram. These can be seen from the Witten diagrams in figure 2. This is manifestly free of any ordering ambiguities since the products of operators that appear can be written in any order. Note that this result can be obtained from flat space Feynman diagrams simply by replacing $2(k_i \cdot k_j)$ with α_{ij}. Similarly, the flat space limit of (A.5) is equivalent to the result given in [89].

B Six-point NLSM from the worldsheet

In this appendix we will compute the six-point wavefunction coefficient of the NLSM in dS using the CSE. For simplicity, we will set the mass and curvature corrections to zero as we did in the previous appendix. The worldsheet calculation turns out to be very intricate and we obtain an expression involving boundary differential operators which do not commute, in contrast to the result of the previous appendix. It is easy to match the two expressions if these commutators are ignored. We therefore expect that the additional terms coming from commutators should cancel out although we have not verified this due to the complexity of the expression. We leave a systematic study of such commutators and potential ordering ambiguities to future work.

By lifting the flat space formula in (2.6) to dS, as explained in section 4, the six-point NLSM wavefunction coefficient in the CSE framework can be written as $\Psi_6^{\mathrm{NLSM}} = \delta^3(\vec{k}_T) A_{\mathrm{NLSM}} \mathcal{C}_6^\Delta$ where

$$
A_{\mathrm{NLSM}} = \int_\gamma \prod_{i=2}^4 d\sigma_i \, (S_i)^{-1} \, (\sigma_{15}\sigma_{56}\sigma_{61})^2 \, \mathrm{PT} \, \frac{1}{\sigma_{15}^2} \, (\mathrm{Pf} A_{15}^{15})^2. \tag{B.1}
$$

Here we have fixed legs $1, 5, 6$ and removed the rows and columns $\{1, 5\}$ from the A-matrix. The contour encircles the poles corresponding to the CSE for legs $2, 3, 4$, i.e. $\gamma \equiv \gamma_{S_2} \cap \gamma_{S_3} \cap \gamma_{S_4}$.

In the following we will focus our attention on A_{NLSM}, which is understood to act on the contact diagram, and impose momentum conservation along the boundary. In order to evaluate the worldsheet integral, we expand $(\text{Pf} A_{15}^{15})^2$ as

$$(\text{Pf} A_{15}^{15})^2 = \frac{\alpha_a}{\sigma_{23}^2 \sigma_{46}^2} + \frac{\alpha_b}{\sigma_{24}^2 \sigma_{36}^2} + \frac{\alpha_c}{\sigma_{26}^2 \sigma_{34}^2} - \text{PT}(2,3,6,4)\,\alpha_d - \text{PT}(2,3,4,6)\,\alpha_e - \text{PT}(2,4,3,6)\,\alpha_f, \tag{B.2}$$

where

$$\alpha_a \equiv \alpha_{23}^2\,\alpha_{46}^2\,, \quad \alpha_b \equiv \alpha_{24}^2\,\alpha_{36}^2\,, \quad \alpha_c \equiv \alpha_{26}^2\,\alpha_{34}^2\,, \quad \alpha_d \equiv \alpha_{23}\,\alpha_{46}\,\alpha_{24}\,\alpha_{36} + \alpha_{24}\,\alpha_{36}\,\alpha_{23}\,\alpha_{46}\,,$$

$$\alpha_e \equiv \alpha_{23}\,\alpha_{46}\,\alpha_{26}\,\alpha_{34} + \alpha_{26}\,\alpha_{34}\,\alpha_{23}\,\alpha_{46}\,, \quad \alpha_f \equiv \alpha_{24}\,\alpha_{36}\,\alpha_{26}\,\alpha_{34} + \alpha_{26}\,\alpha_{34}\,\alpha_{24}\,\alpha_{36}\,, \tag{B.3}$$

and evaluate the integral for each term separately.

Therefore, A_{NLSM} is recast as

$$A_{\text{NLSM}} = \mathcal{A}^{(a)}\alpha_a + \mathcal{A}^{(b)}\alpha_b + \mathcal{A}^{(c)}\alpha_c - \mathcal{A}^{(d)}\alpha_d - \mathcal{A}^{(e)}\alpha_e - \mathcal{A}^{(f)}\alpha_f, \tag{B.4}$$

where we have denoted

$$\mathcal{A}^{(i)} = \int_\gamma \prod_{i=2}^4 \mathrm{d}\sigma_i\,(S_i)^{-1}\,(\sigma_{15}\sigma_{56}\sigma_{61})^2\,\mathcal{I}^{(i)}, \qquad i \in \{a,b,c,d,e,f\}, \tag{B.5}$$

and defined the integrands

$$\mathcal{I}^{(a)} = \text{PT}\,\frac{1}{\sigma_{15}^2\,\sigma_{23}^2\,\sigma_{46}^2}, \qquad \mathcal{I}^{(b)} = \text{PT}\,\frac{1}{\sigma_{15}^2\,\sigma_{24}^2\,\sigma_{36}^2}, \qquad \mathcal{I}^{(c)} = \text{PT}\,\frac{1}{\sigma_{15}^2\,\sigma_{26}^2\,\sigma_{34}^2},$$

$$\mathcal{I}^{(d)} = \text{PT}\,\frac{\text{PT}(2,3,6,4)}{\sigma_{15}^2}, \quad \mathcal{I}^{(e)} = \text{PT}\,\frac{\text{PT}(2,3,4,6)}{\sigma_{15}^2}, \quad \mathcal{I}^{(f)} = \text{PT}\,\frac{\text{PT}(2,4,3,6)}{\sigma_{15}^2}. \tag{B.6}$$

We will evaluate the worldsheet integrals using the graph representation and integration rules introduced in [43, 44]. The graphs corresponding to each term in A_{NLSM} are shown in figure 4. The chords in each circle encode the poles in worldsheet coordinates not contained in the Parke-Taylor factor. For example, $\mathcal{A}^{(a)}$ contains double poles σ_{15}, σ_{23}, and σ_{46} so we draw double lines between these points on the circumference. When evaluating contour integrals, the worldsheet will factorise when a subset of punctures collide. We then draw closed loops around the punctures that collided and refer to them as factorisation cuts. There is a simple set of rules for determining which factorisation cuts contribute:

- *Rule I.* All factorization cuts with fewer than two fixed marked-points (labels with underlines) vanish.

- *Rule II.* If the factorization cuts more than four lines in the corresponding graph then, this contribution vanishes.
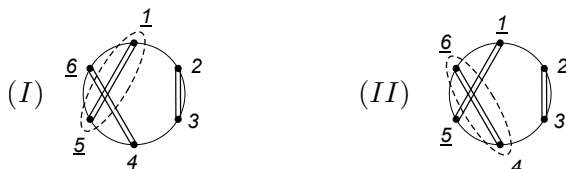
In practice, these rules make calculations much more efficient.

Let us illustrate in detail how to evaluate the first diagram in figure 4. From the integration rules, it is simple to see that there are two factorisation contributions for this
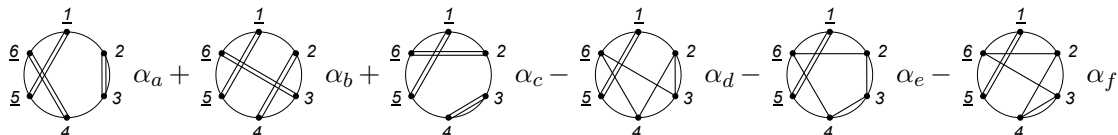
Figure 4. All diagrams for A_{NLSM}.

Figure 5. Factorization contributions for $\mathcal{A}^{(a)}$.

diagram, which are illustrated in figure 5. The contribution (I), is given when $\sigma_2 \to \sigma_3 \to \sigma_4 \to \sigma_6$. To perform this computation, we use the parametrisation, $\sigma_a = \epsilon x_a + \sigma_6$, with $a = 2, 3, 4, 6$, $x_4 = \text{constant}$, $x_6 = 0$, $\sigma_6 = \sigma_L$, and expand around $\epsilon = 0$,

$$\mathrm{d}\sigma_2 \wedge \mathrm{d}\sigma_3 \wedge \mathrm{d}\sigma_4 = \epsilon^2 \, x_{46} \, \mathrm{d}x_2 \wedge \mathrm{d}x_3 \wedge \mathrm{d}\epsilon$$

$$(\sigma_{15}\sigma_{56}\sigma_{61})^2 \, \mathrm{PT} \, \frac{1}{\sigma_{15}^2 \, \sigma_{23}^2 \, \sigma_{46}^2} = \frac{1}{\epsilon^6} \frac{(\sigma_{15}\sigma_{5L}\sigma_{L1})^2}{(\sigma_{L1}^2 \, \sigma_{5L}^2 \, \sigma_{15}^2)} \frac{1}{(x_{23}^2 \, x_{34} \, x_{46}^2)} + \mathcal{O}(\epsilon^{-5}), \tag{B.7}$$

and

$$S_2 = \frac{1}{\epsilon}\left[\hat{S}_2 + \mathcal{O}(\epsilon)\right], \qquad S_3 = \frac{1}{\epsilon}\left[\hat{S}_3 + \mathcal{O}(\epsilon)\right], \qquad S_4 = \frac{1}{\epsilon}\left[\hat{S}_4 + \mathcal{O}(\epsilon)\right],$$

$$\hat{S}_2 = \frac{\alpha_{23}}{x_{23}} + \frac{\alpha_{24}}{x_{24}} + \frac{\alpha_{26}}{x_{26}} + \frac{\alpha_{2R}}{x_{2R}}, \quad \hat{S}_3 = \frac{\alpha_{32}}{x_{32}} + \frac{\alpha_{34}}{x_{34}} + \frac{\alpha_{36}}{x_{36}} + \frac{\alpha_{3R}}{x_{3R}}, \quad \hat{S}_4 = \frac{\alpha_{42}}{x_{42}} + \frac{\alpha_{43}}{x_{43}} + \frac{\alpha_{46}}{x_{46}} + \frac{\alpha_{4R}}{x_{4R}}, \tag{B.8}$$

where $x_R = \infty$, and $\alpha_{aR} = \alpha_{a1} + \alpha_{a5}$, $a = 2, 3, 4$. Now we can deform the contour $\gamma = \gamma_{\hat{S}_2 + \mathcal{O}(\epsilon)} \cap \gamma_{\hat{S}_3 + \mathcal{O}(\epsilon)} \cap \gamma_{\hat{S}_4 + \mathcal{O}(\epsilon)}$ into $\tilde{\gamma} = \gamma_\epsilon \cap \gamma_{\hat{S}_2 + \mathcal{O}(\epsilon)} \cap \gamma_{\hat{S}_3 + \mathcal{O}(\epsilon)}$, where $\gamma_\epsilon = \{|\epsilon| = \delta\}$.

After integrating over γ_ϵ, the full integral is split into two parts: one with $\{\sigma_1, \sigma_5, \sigma_L\}$ and the other with $\{x_2, x_3, x_4, x_6, x_R\}$. Moreover, using the identity

$$\mathrm{PT}(4, 6, R)\,\hat{S}_4 + \mathrm{PT}(3, 6, R)\,\hat{S}_3 + \mathrm{PT}(2, 6, R)\,\hat{S}_2 = \mathrm{PT}(6, R)\,(\alpha_{23} + \alpha_{24} + \alpha_{26} + \alpha_{34} + \alpha_{36} + \alpha_{46}), \tag{B.9}$$

we find that on the support of $\gamma_{\hat{S}_2} \cap \gamma_{\hat{S}_3}$, $\hat{S}_4$ reduces to

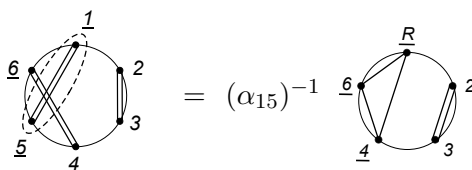$$\hat{S}_4\Big|_{\gamma_{\hat{S}_2} \cap \gamma_{\hat{S}_3}} = \frac{\mathrm{PT}(6, R)}{\mathrm{PT}(4, 6, R)}\,(\alpha_{15}), \tag{B.10}$$

where we have used the CWI. Putting everything together, the contribution (I) for $\mathcal{A}^{(a)}$ is given by

$$\mathcal{A}^{(a)}\Big|_{(I)} = \frac{(\sigma_{15}\sigma_{5L}\sigma_{L1})^2}{(\sigma_{L1}^2\sigma_{5L}^2\sigma_{15}^2)}\,(\alpha_{15})^{-1} \int_{\hat{\gamma}} \prod_{i=2}^{3} \mathrm{d}x_i\,(\hat{S}_i)^{-1}(x_{46}x_{6R}x_{R4})^2 \frac{\mathrm{PT}(2, 3, 4, 6, R)}{x_{23}^2\, x_{46}\, x_{6R}\, x_{R4}}$$

$$= (\alpha_{15})^{-1} \int_{\hat{\gamma}} \prod_{i=2}^{3} \mathrm{d}x_i\,(\hat{S}_i)^{-1}(x_{46}x_{6R}x_{R4})^2 \frac{\mathrm{PT}(2, 3, 4, 6, R)}{x_{23}^2\, x_{46}\, x_{6R}\, x_{R4}}, \tag{B.11}$$

with $\hat{\gamma} = \gamma_{\hat{S}_2} \cap \gamma_{\hat{S}_3}$.

Figure 6. Diagrammatic representation of $\mathcal{A}^{(a)}\big|_{(I)}$.

Figure 7. Factorization contributions for the five-point diagram obtained in $\mathcal{A}^{(a)}\big|_{(I)}$.

The expression in (B.11) is depicted in figure 6. This diagram has two factorisation contributions which are illustrated in figure 7. The contribution $(I\,A)$ arises when $x_2 \to x_3 \to x_4$. In this case we use the parametrisation $x_a = \epsilon\, y_a + x_4$, $a = 2,3,4$, $y_2 =$constant, $y_4 = 0$ and $x_4 = x_L$. We then have

$$\mathrm{d}x_2 \wedge \mathrm{d}x_3 = \epsilon\, y_{24}\, \mathrm{d}\epsilon \wedge \mathrm{d}y_3$$

$$(x_{46}x_{6R}x_{R4})^2\, \frac{\mathrm{PT}(2,3,4,6,R)}{x_{23}^2\, x_{46}\, x_{6R}} = \frac{1}{\epsilon^4}\, \frac{(x_{L6}x_{6R}x_{RL})^2}{(x_{L6}x_{6R}x_{RL})^2}\, \frac{1}{(y_{23}^3\, y_{34})} + \mathcal{O}(\epsilon^{-3}), \qquad (\mathrm{B.12})$$

and

$$\hat{S}_2 = \frac{1}{\epsilon}\left[\tilde{S}_2 + \mathcal{O}(\epsilon)\right], \qquad\qquad \hat{S}_3 = \frac{1}{\epsilon}\left[\tilde{S}_3 + \mathcal{O}(\epsilon)\right],$$

$$\tilde{S}_2 = \frac{\alpha_{23}}{y_{23}} + \frac{\alpha_{24}}{y_{24}} + \frac{\alpha_{2\hat{R}}}{y_{2\hat{R}}}, \qquad\qquad \tilde{S}_3 = \frac{\alpha_{32}}{y_{32}} + \frac{\alpha_{34}}{y_{34}} + \frac{\alpha_{3\hat{R}}}{y_{3\hat{R}}}, \qquad (\mathrm{B.13})$$

where $y_{\hat{R}} = \infty$, and $\alpha_{a\hat{R}} = \alpha_{a1} + \alpha_{a5} + \alpha_{a6}$, $a = 2,3$. By the GRT, we deform the contour $\hat{\gamma} = \gamma_{\tilde{S}_2 + \mathcal{O}(\epsilon)} \cap \gamma_{\tilde{S}_3 + \mathcal{O}(\epsilon)}$ into $\gamma' = -\gamma_\epsilon \cap \gamma_{\tilde{S}_3 + \mathcal{O}(\epsilon)}$. Thus, integrating around $\epsilon = 0$, the five-point integral breaks into two parts: one with $\{x_6, x_R, x_L\}$ and the other with $\{y_2, y_3, y_4, y_{\hat{R}}\}$. Using the identity

$$\mathrm{PT}(2,4,\hat{R})\, \tilde{S}_2 + \mathrm{PT}(3,4,\hat{R})\, \tilde{S}_3 = \mathrm{PT}(4,\hat{R})\left[(\mathcal{D}_2 + \mathcal{D}_3 + \mathcal{D}_4)^2 + m^2\right], \qquad (\mathrm{B.14})$$

we find that on the support of $\gamma_{\tilde{S}_3}$, $\tilde{S}_2$ reduces to

$$\tilde{S}_2\big|_{\gamma_{\tilde{S}_3}} = \frac{\mathrm{PT}(4,\hat{R})}{\mathrm{PT}(2,4,\hat{R})}\left[(\mathcal{D}_2 + \mathcal{D}_3 + \mathcal{D}_4)^2 + m^2\right]. \qquad (\mathrm{B.15})$$

The contribution $(I\,A)$ is therefore given by

$$(I\,A) = \frac{(x_{L6}x_{6R}x_{RL})^2}{(x_{L6}x_{6R}x_{RL})^2}\left[(\mathcal{D}_2 + \mathcal{D}_3 + \mathcal{D}_4)^2 + m^2\right]^{-1}\int_{\gamma_{\tilde{S}_3}} \mathrm{d}y_3(\tilde{S}_3)^{-1}(y_{24}y_{4\hat{R}}y_{\hat{R}2})^2\, \frac{\mathrm{PT}(2,3,4,\hat{R})}{y_{23}^2\, y_{4\hat{R}}^2}$$

$$= \left[(\mathcal{D}_2 + \mathcal{D}_3 + \mathcal{D}_4)^2 + m^2\right]^{-1}\int_{\gamma_{\tilde{S}_3}} \mathrm{d}y_3(\tilde{S}_3)^{-1}(y_{24}y_{4\hat{R}}y_{\hat{R}2})^2\, \frac{\mathrm{PT}(2,3,4,\hat{R})}{y_{23}^2\, y_{4\hat{R}}^2}. \qquad (\mathrm{B.16})$$

Figure 8. Diagramatic representationn for the contribution $(I\,A)$.

The contribution in (B.16) is represented in figure 8. Since the four-point diagram in figure 8 has a double pole, it can potentially give rise to ambiguities associated with the ordering of non-commuting differential operators. In appendix C, we compute this contribution in detail and show that it is well defined. In particular, we find that

$$\int_{\gamma_{\tilde{S}_3}} \mathrm{d}y_3 (\tilde{S}_3)^{-1} (y_{24} y_{4\hat{R}} y_{\hat{R}2})^2 \frac{\mathrm{PT}(2,3,4,\hat{R})}{y_{23}^2 \, y_{4\hat{R}}^2} = (\alpha_{23})^{-1} (\alpha_{23} + \alpha_{34}) (\alpha_{23})^{-1}. \tag{B.17}$$

Plugging this into (B.16) then gives

$$(I\,A) = \left[(\mathcal{D}_2 + \mathcal{D}_3 + \mathcal{D}_4)^2 + m^2 \right]^{-1} (\alpha_{23})^{-1} (\alpha_{23} + \alpha_{34}) (\alpha_{23})^{-1}. \tag{B.18}$$

Similarly, we find the $(I\,B)$ contribution in figure 7 to be

$$(I\,B) = (\alpha_{1235} - \alpha_{15})^{-1} (\alpha_{23})^{-1} (\alpha_{23} + \alpha_{34} + \alpha_{36}) (\alpha_{23})^{-1} \tag{B.19}$$

where $\alpha_{1235} \equiv \alpha_{12} + \alpha_{13} + \alpha_{15} + \alpha_{23} + \alpha_{25} + \alpha_{35}$. Hence, the factorization contribution (I) in figure 5 is given by

$$\mathcal{A}^{(a)}\Big|_{(I)} = (\alpha_{15})^{-1} \left\{ \left[(\mathcal{D}_2 + \mathcal{D}_3 + \mathcal{D}_4)^2 + m^2 \right]^{-1} (\alpha_{23})^{-1} (\alpha_{23} + \alpha_{34}) (\alpha_{23})^{-1} \right.$$
$$\left. + (\alpha_{46} - \alpha_{15})^{-1} (\alpha_{23})^{-1} (\alpha_{23} + \alpha_{34} + \alpha_{36}) (\alpha_{23})^{-1} \right\}. \tag{B.20}$$

The computation for the contribution (II) in figure 5 is completely analogous and we obtain

$$\mathcal{A}^{(a)}\Big|_{(II)} = (\alpha_{46})^{-1} \left\{ \left[(\mathcal{D}_1 + \mathcal{D}_2 + \mathcal{D}_3)^3 + m^2 \right]^{-1} (\alpha_{23})^{-1} (-\alpha_{13}) (\alpha_{23})^{-1} \right.$$
$$\left. + (\alpha_{15} - \alpha_{46})^{-1} (\alpha_{23})^{-1} (\alpha_{23} + \alpha_{34} + \alpha_{36}) (\alpha_{23})^{-1} \right\}. \tag{B.21}$$

Putting it all together, we finally obtain the following formula for the first diagram in figure 4:

$$\mathcal{A}^{(a)} = \mathcal{A}^{(a)}\Big|_{(I)} + \mathcal{A}^{(a)}\Big|_{(II)}$$
$$= \left[(\mathcal{D}_1 + \mathcal{D}_2 + \mathcal{D}_3)^2 + m^2 \right]^{-1} (\alpha_{46})^{-1} (\alpha_{23})^{-1} (-\alpha_{13}) (\alpha_{23})^{-1}$$
$$+ \left[(\mathcal{D}_2 + \mathcal{D}_3 + \mathcal{D}_4)^2 + m^2 \right]^{-1} (\alpha_{15})^{-1} (\alpha_{23})^{-1} (\alpha_{23} + \alpha_{34}) (\alpha_{23})^{-1}$$
$$+ (\alpha_{15})^{-1} (\alpha_{46})^{-1} (\alpha_{23})^{-1} (\alpha_{23} + \alpha_{34} + \alpha_{36}) (\alpha_{23})^{-1}. \tag{B.22}$$
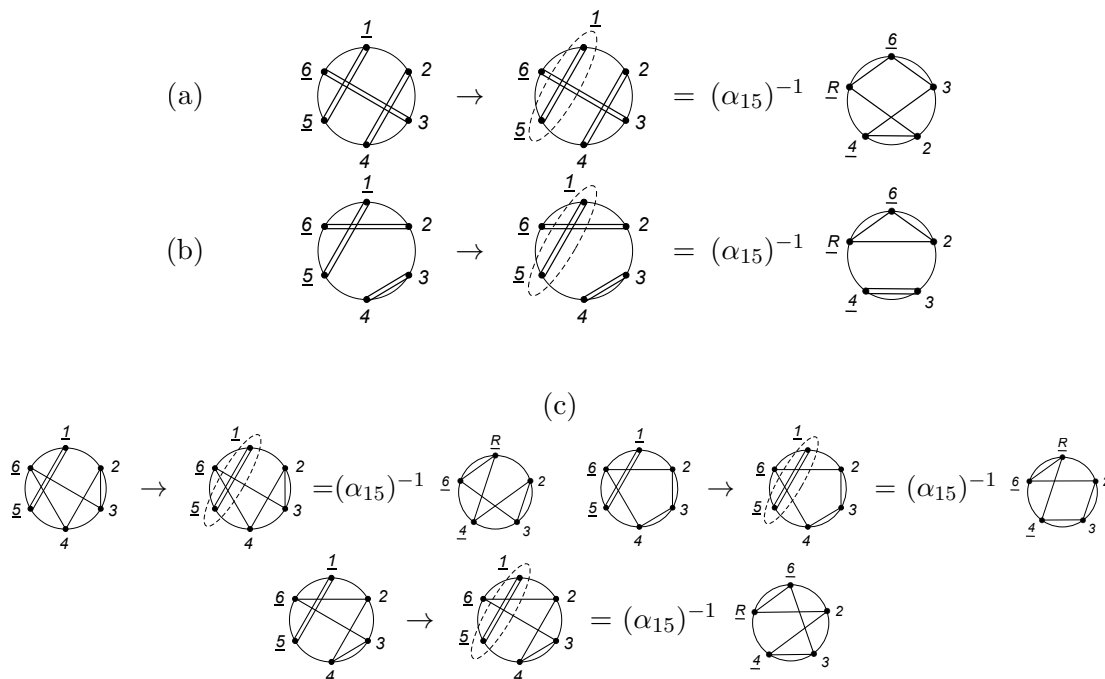
Figure 9. (a) Computing the $\mathcal{A}^{(b)}$ diagram. (b) Computing the $\mathcal{A}^{(c)}$ diagram. (c) Computing the $\mathcal{A}^{(d)}$, $\mathcal{A}^{(e)}$, and $\mathcal{A}^{(f)}$ diagrams.

The other diagrams in figure 4 can be computed using similar methods, so we just state the final results:

$$
\begin{aligned}
\mathcal{A}^{(b)} &= - \left[(\mathcal{D}_2 + \mathcal{D}_3 + \mathcal{D}_4)^2 + m^2 \right]^{-1} (\alpha_{15})^{-1} (\alpha_{24})^{-1} - (\alpha_{15})^{-1} (\alpha_{24})^{-1} (\alpha_{36})^{-1}, \\
\mathcal{A}^{(c)} &= \left[(\mathcal{D}_3 + \mathcal{D}_4 + \mathcal{D}_5)^2 + m^2 \right]^{-1} (\alpha_{26})^{-1} (\alpha_{34})^{-1} (-\alpha_{15}) (\alpha_{34})^{-1} \\
&\quad + \left[(\mathcal{D}_2 + \mathcal{D}_3 + \mathcal{D}_4)^2 + m^2 \right]^{-1} (\alpha_{15})^{-1} (\alpha_{34})^{-1} (\alpha_{23} + \alpha_{34}) (\alpha_{34})^{-1} \\
&\quad + (\alpha_{15})^{-1} (\alpha_{26})^{-1} (\alpha_{34})^{-1} (\alpha_{23} + \alpha_{34} + \alpha_{36}) (\alpha_{34})^{-1}, \\
\mathcal{A}^{(d)} &= \left[(\mathcal{D}_2 + \mathcal{D}_3 + \mathcal{D}_4)^2 + m^2 \right]^{-1} (\alpha_{15})^{-1} (\alpha_{23})^{-1}, \\
\mathcal{A}^{(e)} &= - \left[(\mathcal{D}_2 + \mathcal{D}_3 + \mathcal{D}_4)^2 + m^2 \right]^{-1} (\alpha_{15})^{-1} \left\{ (\alpha_{23})^{-1} + (\alpha_{34})^{-1} \right\}, \\
\mathcal{A}^{(f)} &= \left[(\mathcal{D}_2 + \mathcal{D}_3 + \mathcal{D}_4)^2 + m^2 \right]^{-1} (\alpha_{15})^{-1} (\alpha_{34})^{-1}.
\end{aligned}
\tag{B.23}
$$

The factorisation cuts from which these were derived are illustrated in figure 9. The complete result is then obtained by combining (B.22) with (B.23). Neglecting commutators, it is not difficult to see that this agrees with (A.5).

C Four-point diagram with double pole

In this appendix, we will illustrate how to evaluate a worldsheet integral with a double pole. This integral arises in the 6-point NLSM computation as explained in the previous
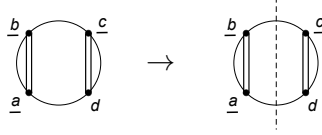
Figure 10. Four-point diagrams with double pole and its factorisation contribution.

appendix. Non-simple poles can also appear in four-point worldsheet formulae of higher-derivative theories like DBI and sGal, as explained in section 4, although they can be avoided using an appropriate choice of Pfaffians. Let us consider the integral

$$\mathcal{A}_4 = \int_{\gamma_{S_d}} \mathrm{d}\sigma_d \, (S_d)^{-1} (\sigma_{ab}\sigma_{bc}\sigma_{ca})^2 \, \mathrm{PT}(a,b,c,d) \, \frac{1}{\sigma_{ab}^2 \sigma_{cd}^2}, \tag{C.1}$$

where

$$S_d = \frac{\alpha_{da}}{\sigma_{da}} + \frac{\alpha_{db}}{\sigma_{db}} + \frac{\alpha_{dc}}{\sigma_{dc}}, \tag{C.2}$$

and $\alpha_{da} + \alpha_{db} + \alpha_{dc} = 0$ when acting on a four-point contact diagram with $\mathcal{D}_a^2 \neq \mathcal{D}_b^2 \neq \mathcal{D}_c^2 \neq -m^2$ (see section 6.2 of [44] for a discussion of how CWI and $\mathrm{SL}(2,\mathbb{C})$ symmetry are realised in this context).

In the following, it will be understood that $\mathcal{A}_4$ acts on a contact diagram and that momentum in conserved along the boundary. In figure 10, we give the graph representation for $\mathcal{A}_4$ and its factorisation contribution after applying the integration rules reviewed in the previous appendix. This factorisation contribution is given when $\sigma_d \to \sigma_c$. To carry out this computation we use the parametrisation $\sigma_i = \epsilon x_i + \sigma_c$, with $i = c, d$, $x_d = \text{constant}$, $x_c = 0$, $\sigma_c = \sigma_L$, and expand around $\epsilon = 0$:

$$\mathrm{d}\sigma_d = x_{dc} \, \mathrm{d}\epsilon$$

$$(\sigma_{ab}\sigma_{bc}\sigma_{ca})^2 \, \mathrm{PT}(a,b,c,d) \, \frac{1}{\sigma_{ab}^2 \sigma_{cd}^2} = \frac{1}{\epsilon^3} \frac{(\sigma_{ab}\sigma_{bL}\sigma_{La})^2}{(\sigma_{ab}^3 \sigma_{bL} \, \sigma_{La} \, x_{cd}^3)} \left(1 + \epsilon \frac{x_{cd}}{\sigma_{La}} + \mathcal{O}(\epsilon^2) \right), \tag{C.3}$$

and

$$S_d = \frac{1}{\epsilon} \left[\hat{S}_d(\epsilon) + \mathcal{O}(\epsilon^2) \right], \qquad \hat{S}_d(\epsilon) \equiv \frac{\alpha_{dc}}{x_{dc}} + \epsilon \left(\frac{\alpha_{da}}{\sigma_{La}} + \frac{\alpha_{db}}{\sigma_{Lb}} \right). \tag{C.4}$$

Using the global residue theorem, the integral becomes an integration around $\epsilon = 0$, i.e.

$$\mathcal{A}_4 = \int_{\gamma_\epsilon} \frac{\mathrm{d}\epsilon}{\epsilon} \left[\hat{S}_d(\epsilon) + \mathcal{O}(\epsilon^2) \right]^{-1} \frac{\sigma_{bL}}{(\sigma_{ab} \, x_{cd})} + \int_{\gamma_\epsilon} \frac{\mathrm{d}\epsilon}{\epsilon^2} \left[\hat{S}_d(\epsilon) + \mathcal{O}(\epsilon^2) \right]^{-1} \frac{(\sigma_{bL}\sigma_{La})}{(\sigma_{ab} \, x_{cd}^2)}. \tag{C.5}$$

The first term has a simple pole and is simple to evaluate

$$\int_{\gamma_\epsilon} \frac{\mathrm{d}\epsilon}{\epsilon} \left[\hat{S}_d(\epsilon) + \mathcal{O}(\epsilon^2) \right]^{-1} \frac{\sigma_{bL}}{(\sigma_{ab} \, x_{cd})} = -\frac{\sigma_{bL}}{\sigma_{ab}} \, (\alpha_{dc})^{-1}. \tag{C.6}$$

Since the second term in (C.5) has a double pole, we must compute the derivative $\frac{\mathrm{d}[(\hat{S}_d(\epsilon))^{-1}]}{\mathrm{d}\epsilon}$, which must be done with care since $\hat{S}_d$ is a differential operator. Using the identity

$$\hat{S}_d(\epsilon) \, [\hat{S}_d(\epsilon)]^{-1} = \mathbb{I}, \tag{C.7}$$

it is straightforward to arrive at the following result:

$$\frac{\mathrm{d}[(\hat{S}_d(\epsilon))^{-1}]}{\mathrm{d}\epsilon}\Big|_{\epsilon=0} = -[\hat{S}_d(0)]^{-1}\hat{S}_d'(0)\,[\hat{S}_d(0)]^{-1} = -x_{dc}^2\,(\alpha_{dc})^{-1}\left(\frac{\alpha_{da}}{\sigma_{La}} + \frac{\alpha_{db}}{\sigma_{Lb}}\right)(\alpha_{dc})^{-1}.$$

(C.8)

Therefore, the second integral in (C.5) is given by

$$\int_{\gamma_\epsilon} \frac{\mathrm{d}\epsilon}{\epsilon^2}\left[\hat{S}_d(\epsilon) + \mathcal{O}(\epsilon^2)\right]^{-1}\frac{(\sigma_{bL}\sigma_{La})}{(\sigma_{ab}\ x_{cd}^2)} = \frac{1}{\sigma_{ab}}(\alpha_{dc})^{-1}\,(\sigma_{Lb}\,\alpha_{da} + \sigma_{La}\,\alpha_{db})\,(\alpha_{dc})^{-1}.$$

(C.9)

Finally, we obtain

$$\begin{aligned}
\mathcal{A}_4 &= \frac{1}{\sigma_{ab}}(\alpha_{dc})^{-1}\,(\sigma_{Lb}\,\alpha_{dc} + \sigma_{Lb}\,\alpha_{da} + \sigma_{La}\,\alpha_{db})\,(\alpha_{dc})^{-1}\\
&= -(\alpha_{cd})^{-1}(\alpha_{db})(\alpha_{cd})^{-1}\\
&= (\alpha_{cd})^{-1}(\alpha_{ad} + \alpha_{cd})(\alpha_{cd})^{-1},
\end{aligned}$$

(C.10)

where we have used the CWI in (C.2) in the last two lines.

D Six-derivative results

For minimally coupled scalars we find that

$$(\hat{s}^3 + \hat{t}^3 + \hat{u}^3)\mathcal{C}_4^{\Delta=3}$$

$$= \frac{360}{E^7}k_1k_2k_3k_4k_1^\mu k_{2,\mu}k_3^\nu k_{4,\nu}\,(k_1^\sigma k_{2,\sigma} + k_3^\sigma k_{4,\sigma})\left(1 + \frac{E}{6}\sum_{i=1}^4\frac{1}{k_i} + \frac{E^2}{30k_1k_2k_3k_4}\sum_{i<j}k_ik_j\right)$$

$$+ \frac{60}{E^6}k_1k_2k_3k_4\left((k_3 + k_4)(k_1^\mu k_{2,\mu})^2 + (k_1 + k_2)(k_3^\mu k_{4,\mu})^2\right)$$

$$+ \frac{24}{E^5}\Bigg(10k_1k_2k_3k_4k_1^\mu k_{2,\mu}k_3^\nu k_{4,\nu}$$

$$+ \frac{1}{2}\sum_{i<j}k_ik_j\Big(2k_1k_2k_3k_4\,(k_1^\mu k_{2,\mu} + k_3^\mu k_{4,\mu} - k_1k_2 - k_3k_4) - 2k_3^2k_4^2k_1^\mu k_{2,\mu}$$

$$- 2k_1^2k_2^2k_3^\mu k_{4,\mu} + 2(k_1k_2 + k_3k_4)k_1^\mu k_{2,\mu}k_3^\nu k_{4,\nu} + k_3k_4(k_1^\mu k_{2,\mu})^2$$

$$+ k_1k_2(k_3^\mu k_{4,\mu})^2\Big) + \left(1 + \sum_{i\neq j}\frac{k_i}{k_j}\right)k_1k_2k_3k_4\vec{k}_1\cdot\vec{k}_2\vec{k}_3\cdot\vec{k}_4$$

$$- (k_1^2k_2^2 + k_3^2k_4^2)\vec{k}_1\cdot\vec{k}_2\vec{k}_3\cdot\vec{k}_4 + k_3^2k_4^2\vec{k}_1\cdot\vec{k}_2\left(-k_1^2 - k_2^2 + 2(k_1k_2 + k_3k_4)\right)$$

$$+ k_1^2k_2^2\vec{k}_3\cdot\vec{k}_4\left(-k_3^2 - k_4^2 + 2(k_1k_2 + k_3k_4)\right)$$

$$- \frac{1}{2}\left(4k_1^2k_2^2k_3^2k_4^2 + k_1^2k_2^2(\vec{k}_3\cdot\vec{k}_4)^2 + (\vec{k}_1\cdot\vec{k}_2)^2\right)\Bigg)$$

$$+ \frac{6}{E^4}\Bigg(\left(\left(k_1k_2k_3k_4\sum_{i=1}^4\frac{1}{k_i} + \sum_{i\neq j}k_ik_j^2\right)\vec{k}_1\cdot\vec{k}_2\vec{k}_3\cdot\vec{k}_4\right.$$

$$- 2k_3^2k_4^2(k_3 + k_4)\vec{k}_1\cdot\vec{k}_2 - 2k_1^2k_2^2(k_1 + k_2)\vec{k}_3\cdot\vec{k}_4\Bigg)$$

$$+ \frac{2}{E^3} \Bigg(2\vec{k}_1 \cdot \vec{k}_2 \vec{k}_3 \cdot \vec{k}_4 (\vec{k}_1 \cdot \vec{k}_2 + \vec{k}_3 \cdot \vec{k}_4) - \sum_{i<j} k_i k_j \vec{k}_1 \cdot \vec{k}_2 \vec{k}_3 \cdot \vec{k}_4$$

$$+ 2k_3^2 k_4^2 \vec{k}_1 \cdot \vec{k}_2 + 2k_1^2 k_2^2 \vec{k}_3 \cdot \vec{k}_4 \Bigg)$$

$$+ \frac{4}{E} \vec{k}_1 \cdot \vec{k}_2 \vec{k}_3 \cdot \vec{k}_4 + \text{Cyc}.[234], \tag{D.1}$$

where $k_i^\mu k_{j,\mu} = \vec{k}_i \cdot \vec{k}_j - k_i k_j$. This expression mixes different types of dot products in order to obtain a more compact form.

References

[1] A.H. Guth, *The Inflationary Universe: A Possible Solution to the Horizon and Flatness Problems*, *Phys. Rev. D* **23** (1981) 347 [INSPIRE].

[2] A.D. Linde, *A New Inflationary Universe Scenario: A Possible Solution of the Horizon, Flatness, Homogeneity, Isotropy and Primordial Monopole Problems*, *Phys. Lett. B* **108** (1982) 389 [INSPIRE].

[3] A. Albrecht and P.J. Steinhardt, *Cosmology for Grand Unified Theories with Radiatively Induced Symmetry Breaking*, *Phys. Rev. Lett.* **48** (1982) 1220 [INSPIRE].

[4] V.F. Mukhanov and G.V. Chibisov, *Quantum Fluctuations and a Nonsingular Universe*, *JETP Lett.* **33** (1981) 532 [INSPIRE].

[5] J.B. Hartle and S.W. Hawking, *Wave Function of the Universe*, *Phys. Rev. D* **28** (1983) 2960 [INSPIRE].

[6] A. Strominger, *Inflation and the dS/CFT correspondence*, *JHEP* **11** (2001) 049 [hep-th/0110087] [INSPIRE].

[7] J.M. Maldacena, *Non-Gaussian features of primordial fluctuations in single field inflationary models*, *JHEP* **05** (2003) 013 [astro-ph/0210603] [INSPIRE].

[8] P. McFadden and K. Skenderis, *Holography for Cosmology*, *Phys. Rev. D* **81** (2010) 021301 [arXiv:0907.5542] [INSPIRE].

[9] P. McFadden and K. Skenderis, *Holographic Non-Gaussianity*, *JCAP* **05** (2011) 013 [arXiv:1011.0452] [INSPIRE].

[10] J.M. Maldacena and G.L. Pimentel, *On graviton non-Gaussianities during inflation*, *JHEP* **09** (2011) 045 [arXiv:1104.2846] [INSPIRE].

[11] S. Raju, *Recursion Relations for AdS/CFT Correlators*, *Phys. Rev. D* **83** (2011) 126002 [arXiv:1102.4724] [INSPIRE].

[12] A. Ghosh, N. Kundu, S. Raju and S.P. Trivedi, *Conformal Invariance and the Four Point Scalar Correlator in Slow-Roll Inflation*, *JHEP* **07** (2014) 011 [arXiv:1401.1426] [INSPIRE].

[13] S. Weinberg, *Quantum contributions to cosmological correlations*, *Phys. Rev. D* **72** (2005) 043514 [hep-th/0506236] [INSPIRE].

[14] N. Arkani-Hamed, P. Benincasa and A. Postnikov, *Cosmological Polytopes and the Wavefunction of the Universe*, arXiv:1709.02813 [INSPIRE].

[15] A. Bzowski, P. McFadden and K. Skenderis, *Conformal correlators as simplex integrals in momentum space*, *JHEP* **01** (2021) 192 [arXiv:2008.07543] [INSPIRE].

[16] N. Arkani-Hamed and J. Maldacena, *Cosmological Collider Physics*, arXiv:1503.08043 [INSPIRE].

[17] N. Arkani-Hamed, D. Baumann, H. Lee and G.L. Pimentel, *The Cosmological Bootstrap: Inflationary Correlators from Symmetries and Singularities*, *JHEP* **04** (2020) 105 [arXiv:1811.00024] [INSPIRE].

[18] D. Baumann, C. Duaso Pueyo, A. Joyce, H. Lee and G.L. Pimentel, *The cosmological bootstrap: weight-shifting operators and scalar seeds*, *JHEP* **12** (2020) 204 [arXiv:1910.14051] [INSPIRE].

[19] D. Baumann, C. Duaso Pueyo, A. Joyce, H. Lee and G.L. Pimentel, *The Cosmological Bootstrap: Spinning Correlators from Symmetries and Factorization*, *SciPost Phys.* **11** (2021) 071 [arXiv:2005.04234] [INSPIRE].

[20] D. Baumann, W.-M. Chen, C. Duaso Pueyo, A. Joyce, H. Lee and G.L. Pimentel, *Linking the Singularities of Cosmological Correlators*, arXiv:2106.05294 [INSPIRE].

[21] D. Meltzer, *The inflationary wavefunction from analyticity and factorization*, *JCAP* **12** (2021) 018 [arXiv:2107.10266] [INSPIRE].

[22] A. Hillman and E. Pajer, *A differential representation of cosmological wavefunctions*, *JHEP* **04** (2022) 012 [arXiv:2112.01619] [INSPIRE].

[23] L.F. Alday and S. Caron-Huot, *Gravitational S-matrix from CFT dispersion relations*, *JHEP* **12** (2018) 017 [arXiv:1711.02031] [INSPIRE].

[24] D. Meltzer and A. Sivaramakrishnan, *CFT unitarity and the AdS Cutkosky rules*, *JHEP* **11** (2020) 073 [arXiv:2008.11730] [INSPIRE].

[25] H. Goodhew, S. Jazayeri and E. Pajer, *The Cosmological Optical Theorem*, *JCAP* **04** (2021) 021 [arXiv:2009.02898] [INSPIRE].

[26] S. Melville and E. Pajer, *Cosmological Cutting Rules*, *JHEP* **05** (2021) 249 [arXiv:2103.09832] [INSPIRE].

[27] S. Jazayeri, E. Pajer and D. Stefanyszyn, *From locality and unitarity to cosmological correlators*, *JHEP* **10** (2021) 065 [arXiv:2103.08649] [INSPIRE].

[28] H. Goodhew, S. Jazayeri, M.H. Gordon Lee and E. Pajer, *Cutting cosmological correlators*, *JCAP* **08** (2021) 003 [arXiv:2104.06587] [INSPIRE].

[29] C. Sleight and M. Taronna, *Bootstrapping Inflationary Correlators in Mellin Space*, *JHEP* **02** (2020) 098 [arXiv:1907.01143] [INSPIRE].

[30] C. Sleight and M. Taronna, *From dS to AdS and back*, *JHEP* **12** (2021) 074 [arXiv:2109.02725] [INSPIRE].

[31] C. Armstrong, A.E. Lipstein and J. Mei, *Color/kinematics duality in AdS$_4$*, *JHEP* **02** (2021) 194 [arXiv:2012.02059] [INSPIRE].

[32] S. Albayrak, S. Kharel and D. Meltzer, *On duality of color and kinematics in (A)dS momentum space*, *JHEP* **03** (2021) 249 [arXiv:2012.10460] [INSPIRE].

[33] L.F. Alday, C. Behan, P. Ferrero and X. Zhou, *Gluon Scattering in AdS from CFT*, *JHEP* **06** (2021) 020 [arXiv:2103.15830] [INSPIRE].

[34] P. Diwakar, A. Herderschee, R. Roiban and F. Teng, *BCJ amplitude relations for Anti-de Sitter boundary correlators in embedding space*, *JHEP* **10** (2021) 141 [arXiv:2106.10822] [INSPIRE].

[35] A. Sivaramakrishnan, *Towards color-kinematics duality in generic spacetimes*, *JHEP* **04** (2022) 036 [arXiv:2110.15356] [INSPIRE].

[36] C. Cheung, J. Parra-Martinez and A. Sivaramakrishnan, *On-shell correlators and color-kinematics duality in curved symmetric spacetimes*, *JHEP* **05** (2022) 027 [arXiv:2201.05147] [INSPIRE].

[37] A. Herderschee, R. Roiban and F. Teng, *On the differential representation and color-kinematics duality of AdS boundary correlators*, *JHEP* **05** (2022) 026 [arXiv:2201.05067] [INSPIRE].

[38] J.M. Drummond, R. Glew and M. Santagata, *BCJ relations in $AdS_5 \times S^3$ and the double-trace spectrum of super gluons*, arXiv:2202.09837 [INSPIRE].

[39] J.A. Farrow, A.E. Lipstein and P. McFadden, *Double copy structure of CFT correlators*, *JHEP* **02** (2019) 130 [arXiv:1812.11129] [INSPIRE].

[40] A.E. Lipstein and P. McFadden, *Double copy structure and the flat space limit of conformal correlators in even dimensions*, *Phys. Rev. D* **101** (2020) 125006 [arXiv:1912.10046] [INSPIRE].

[41] S. Jain, R.R. John, A. Mehta, A.A. Nizami and A. Suresh, *Double copy structure of parity-violating CFT correlators*, *JHEP* **07** (2021) 033 [arXiv:2104.12803] [INSPIRE].

[42] X. Zhou, *Double Copy Relation in AdS Space*, *Phys. Rev. Lett.* **127** (2021) 141601 [arXiv:2106.07651] [INSPIRE].

[43] H. Gomez, R.L. Jusinskas and A. Lipstein, *Cosmological Scattering Equations*, *Phys. Rev. Lett.* **127** (2021) 251604 [arXiv:2106.11903] [INSPIRE].

[44] H. Gomez, R. Lipinski Jusinskas and A. Lipstein, *Cosmological scattering equations at tree-level and one-loop*, *JHEP* **07** (2022) 004 [arXiv:2112.12695] [INSPIRE].

[45] S. Fichet, *On Holography in General Background and the Boundary Effective Action from AdS to dS*, arXiv:2112.00746 [INSPIRE].

[46] A. Herderschee, *A New Framework for Higher Loop Witten Diagrams*, arXiv:2112.08226 [INSPIRE].

[47] A. Gadde and T. Sharma, *A Scattering Amplitude for Massive Particles in AdS*, arXiv:2204.06462 [INSPIRE].

[48] T. Heckelbacher, I. Sachs, E. Skvortsov and P. Vanhove, *Analytical evaluation of cosmological correlation functions*, arXiv:2204.07217 [INSPIRE].

[49] Z. Bern, J.J.M. Carrasco and H. Johansson, *New Relations for Gauge-Theory Amplitudes*, *Phys. Rev. D* **78** (2008) 085011 [arXiv:0805.3993] [INSPIRE].

[50] Z. Bern, J.J.M. Carrasco and H. Johansson, *Perturbative Quantum Gravity as a Double Copy of Gauge Theory*, *Phys. Rev. Lett.* **105** (2010) 061602 [arXiv:1004.0476] [INSPIRE].

[51] D.B. Fairlie and D.E. Roberts, *Dual models without tachyons — A new approach*, PRINT-72-2440 (1972) [InSPIRE].

[52] D.J. Gross and P.F. Mende, *The High-Energy Behavior of String Scattering Amplitudes*, *Phys. Lett. B* **197** (1987) 129 [InSPIRE].

[53] F. Cachazo, S. He and E.Y. Yuan, *Scattering of Massless Particles in Arbitrary Dimensions*, *Phys. Rev. Lett.* **113** (2014) 171601 [arXiv:1307.2199] [InSPIRE].

[54] F. Cachazo, S. He and E.Y. Yuan, *Scattering of Massless Particles: Scalars, Gluons and Gravitons*, *JHEP* **07** (2014) 033 [arXiv:1309.0885] [InSPIRE].

[55] L. Mason and D. Skinner, *Ambitwistor strings and the scattering equations*, *JHEP* **07** (2014) 048 [arXiv:1311.2564] [InSPIRE].

[56] F. Cachazo, S. He and E.Y. Yuan, *Scattering Equations and Matrices: From Einstein To Yang-Mills, DBI and NLSM*, *JHEP* **07** (2015) 149 [arXiv:1412.3479] [InSPIRE].

[57] E. Casali, Y. Geyer, L. Mason, R. Monteiro and K.A. Roehrig, *New Ambitwistor String Theories*, *JHEP* **11** (2015) 038 [arXiv:1506.08771] [InSPIRE].

[58] C. Cheung, C.-H. Shen and C. Wen, *Unifying Relations for Scattering Amplitudes*, *JHEP* **02** (2018) 095 [arXiv:1705.03025] [InSPIRE].

[59] L. Eberhardt, S. Komatsu and S. Mizera, *Scattering equations in AdS: scalar correlators in arbitrary dimensions*, *JHEP* **11** (2020) 158 [arXiv:2007.06574] [InSPIRE].

[60] K. Roehrig and D. Skinner, *Ambitwistor strings and the scattering equations on $AdS_3 \times S^3$*, *JHEP* **02** (2022) 073 [arXiv:2007.07234] [InSPIRE].

[61] S.L. Adler, *Consistency conditions on the strong interactions implied by a partially conserved axial vector current*, *Phys. Rev.* **137** (1965) B1022 [InSPIRE].

[62] C. Cheung, K. Kampf, J. Novotny and J. Trnka, *Effective Field Theories from Soft Limits of Scattering Amplitudes*, *Phys. Rev. Lett.* **114** (2015) 221602 [arXiv:1412.4095] [InSPIRE].

[63] I. Low, *Adler's zero and effective Lagrangians for nonlinearly realized symmetry*, *Phys. Rev. D* **91** (2015) 105017 [arXiv:1412.2145] [InSPIRE].

[64] K. Hinterbichler and A. Joyce, *Hidden symmetry of the Galileon*, *Phys. Rev. D* **92** (2015) 023503 [arXiv:1501.07600] [InSPIRE].

[65] A. Padilla, D. Stefanyszyn and T. Wilson, *Probing Scalar Effective Field Theories with the Soft Limits of Scattering Amplitudes*, *JHEP* **04** (2017) 015 [arXiv:1612.04283] [InSPIRE].

[66] J. Bonifacio, K. Hinterbichler, A. Joyce and D. Roest, *Exceptional scalar theories in de Sitter space*, *JHEP* **04** (2022) 128 [arXiv:2112.12151] [InSPIRE].

[67] N. Bittermann and A. Joyce, *Soft limits of the wavefunction in exceptional scalar theories*, arXiv:2203.05576 [InSPIRE].

[68] N.E.J. Bjerrum-Bohr, J.L. Bourjaily, P.H. Damgaard and B. Feng, *Manifesting Color-Kinematics Duality in the Scattering Equation Formalism*, *JHEP* **09** (2016) 094 [arXiv:1608.00006] [InSPIRE].

[69] C.-H. Fu, Y.-J. Du, R. Huang and B. Feng, *Expansion of Einstein-Yang-Mills Amplitude*, *JHEP* **09** (2017) 021 [arXiv:1702.08158] [InSPIRE].

[70] A. Edison and F. Teng, *Efficient Calculation of Crossing Symmetric BCJ Tree Numerators*, *JHEP* **12** (2020) 138 [arXiv:2005.03638] [InSPIRE].

[71] N.E.J. Bjerrum-Bohr, T.V. Brown and H. Gomez, *Scattering of Gravitons and Spinning Massive States from Compact Numerators*, *JHEP* **04** (2021) 234 [arXiv:2011.10556] [INSPIRE].

[72] I. Low, L. Rodina and Z. Yin, *Double Copy in Higher Derivative Operators of Nambu-Goldstone Bosons*, *Phys. Rev. D* **103** (2021) 025004 [arXiv:2009.00008] [INSPIRE].

[73] I. Heemskerk, J. Penedones, J. Polchinski and J. Sully, *Holography from Conformal Field Theory*, *JHEP* **10** (2009) 079 [arXiv:0907.0151] [INSPIRE].

[74] L. Dolan and P. Goddard, *Proof of the Formula of Cachazo, He and Yuan for Yang-Mills Tree Amplitudes in Arbitrary Dimension*, *JHEP* **05** (2014) 010 [arXiv:1311.5200] [INSPIRE].

[75] P. Creminelli, J. Noreña and M. Simonović, *Conformal consistency relations for single-field inflation*, *JCAP* **07** (2012) 052 [arXiv:1203.4595] [INSPIRE].

[76] K. Hinterbichler, L. Hui and J. Khoury, *An Infinite Set of Ward Identities for Adiabatic Modes in Cosmology*, *JCAP* **01** (2014) 039 [arXiv:1304.5527] [INSPIRE].

[77] N. Kundu, A. Shukla and S.P. Trivedi, *Constraints from Conformal Symmetry on the Three Point Scalar Correlator in Inflation*, *JHEP* **04** (2015) 061 [arXiv:1410.2606] [INSPIRE].

[78] P. Creminelli, *On non-Gaussianities in single-field inflation*, *JCAP* **10** (2003) 003 [astro-ph/0306122] [INSPIRE].

[79] V. Assassi, D. Baumann and D. Green, *On Soft Limits of Inflationary Correlation Functions*, *JCAP* **11** (2012) 047 [arXiv:1204.4207] [INSPIRE].

[80] N. Kundu, A. Shukla and S.P. Trivedi, *Ward Identities for Scale and Special Conformal Transformations in Inflation*, *JHEP* **01** (2016) 046 [arXiv:1507.06017] [INSPIRE].

[81] A. Shukla, S.P. Trivedi and V. Vishal, *Symmetry constraints in inflation, α-vacua, and the three point function*, *JHEP* **12** (2016) 102 [arXiv:1607.08636] [INSPIRE].

[82] A. Bzowski, P. McFadden and K. Skenderis, *Scalar 3-point functions in CFT: renormalisation, β-functions and anomalies*, *JHEP* **03** (2016) 066 [arXiv:1510.08442] [INSPIRE].

[83] A. Bzowski, P. McFadden and K. Skenderis, *Renormalised 3-point functions of stress tensors and conserved currents in CFT*, *JHEP* **11** (2018) 153 [arXiv:1711.09105] [INSPIRE].

[84] A. Bzowski, P. McFadden and K. Skenderis, *Renormalised CFT 3-point functions of scalars, currents and stress tensors*, *JHEP* **11** (2018) 159 [arXiv:1805.12100] [INSPIRE].

[85] A. Bzowski, P. McFadden and K. Skenderis, *Handbook of holographic 4-point functions*, to appear.

[86] C. Cheung, P. Creminelli, A.L. Fitzpatrick, J. Kaplan and L. Senatore, *The Effective Field Theory of Inflation*, *JHEP* **03** (2008) 014 [arXiv:0709.0293] [INSPIRE].

[87] D. Green and E. Pajer, *On the Symmetries of Cosmological Perturbations*, *JCAP* **09** (2020) 032 [arXiv:2004.09587] [INSPIRE].

[88] E. Pajer, *Building a Boostless Bootstrap for the Bispectrum*, *JCAP* **01** (2021) 023 [arXiv:2010.12818] [INSPIRE].

[89] K. Kampf, J. Novotny and J. Trnka, *Tree-level Amplitudes in the Nonlinear Sigma Model*, *JHEP* **05** (2013) 032 [arXiv:1304.3048] [INSPIRE].